

# Discovering Potent Inhibitors Against the $\beta$ -Hydroxyacyl-Acyl Carrier Protein Dehydratase (FabZ) of *Helicobacter pylori*: Structure-Based Design, Synthesis, Bioassay, and Crystal Structure Determination<sup>†</sup>

Lingyan He,<sup>‡,§</sup> Liang Zhang,<sup>‡,§</sup> Xiaofeng Liu,<sup>‡,§</sup> Xianghua Li,<sup>§</sup> Mingyue Zheng,<sup>§</sup> Honglin Li,<sup>§</sup> Kunqian Yu,<sup>§</sup> Kaixian Chen,<sup>§</sup> Xu Shen,<sup>\*,§,||</sup> Hualiang Jiang,<sup>\*,§,||</sup> and Hong Liu<sup>\*,§</sup>

Center for Drug Discovery and Design, State Key Laboratory of Drug Research, Shanghai Institute of Materia Medica, Chinese Academy of Sciences, 555 Zuchongzhi Road, Shanghai 201203, China, School of Pharmacy, East China University of Science and Technology, Shanghai 200237, China

Received December 10, 2008

The discovery of *HpFabZ* inhibitors is now of special interest in the treatment of various gastric diseases. In this work, three series of derivatives (compounds **3**, **4**, and **5**) were designed, synthesized, and their biological activities were investigated as potential *HpFabZ* inhibitors in a two phased manner. First, we designed and synthesized two series of derivatives (**3a–r** and **4a–u**) and evaluated the enzyme-based assay against *HpFabZ*. Five compounds (**3i–k**, **3m**, and **3q**) showed potential inhibitory activity, with IC<sub>50</sub> values less than 2  $\mu$ M. Second, a focused combinatorial library containing 280 molecules was designed employing the LD1.0 program. Twelve compounds (**5a–l**) were selected and synthesized. The activity of the most potent compound **5h** (IC<sub>50</sub> = 0.86  $\mu$ M) was 46 times higher than that of the hit **1**. The high hit rate and the potency of the new *HpFabZ* inhibitors demonstrated the efficiency of the strategy for the focused library design and virtual screening.

## 1. Introduction

*Helicobacter pylori* (*H. pylori*<sup>a</sup>) has recently been the subject of intense interest because it is a major causative factor for gastrointestinal illnesses such as chronic gastritis and peptic ulcers.<sup>1–5</sup> Additionally, infection of *H. pylori* is also associated with adenocarcinomas and stomach lymphomas, increasing the risk of gastric cancer.<sup>6,7</sup> Nevertheless, there is no effective therapy in eradicating *H. pylori* infection. Combination therapies employing one proton pump inhibitor (e.g., omeprazole) and two or three antibiotics (e.g., amoxicillin, clarithromycin, or tetracycline) have been used as preferred treatments.<sup>8–10</sup> However, the multiple therapy regimens have not been very effective in the clinical setting because the bacterium is likely to develop resistance.<sup>11–14</sup> Moreover, this treatment may disrupt the natural population of commensal microorganisms in the gastrointestinal tract, leading to undesired side effects such as diarrhea.<sup>15,16</sup> Hence, a new level of treatment is needed to inactivate the key enzymes associated with the bacterial growth.

Recently, the pathway of the type-II fatty acid biosynthesis system (FAS-II) has been particularly appreciated as an interest-

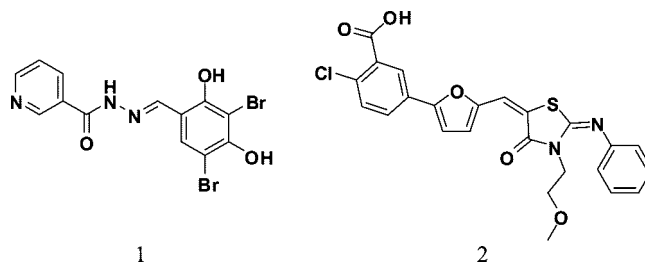


Figure 1. The structures of compounds **1** and **2**.

ing target for antibacterial agent discovery due to the major differences of the structural architectures and biological functions that exist between the plastid-associated enzymes of FAS-II found in most microorganisms and the enzymes involved in FAS-I for mammals and yeast.<sup>17–20</sup> FAS-II consists of six key enzymes: FabD, FabH, FabF (or FabB), FabI, FabZ (or FabA), and FabG, all of which work in concert during the synthesis of fatty acid in vivo including the initiation and elongation phases. During the elongation cycle of FAS II, four consecutive reactions complete the extension of two carbons.<sup>21,22</sup> In the third step of the elongation cycle, the dehydration of  $\beta$ -hydroxy-ACP to *trans*-2-acyl-ACP is catalyzed by FabZ or FabA. FabA is a bifunctional enzyme and is only found in Gram-negative bacteria with its partner, FabB, to participate in the formation of unsaturated fatty acids.<sup>23</sup> However, FabZ has a ubiquitous distribution in the FAS II pathway and is a primary dehydratase that participates in the elongation cycles of both saturated and unsaturated fatty acid biosyntheses. Accordingly, FabZ presents itself as a suitable, yet unexplored target for the discovery of compounds against pathogenic microbes.<sup>22,23</sup>

So far, the only known small molecule inhibitors of FabZ are flavonoids discovered by random screening against *Plasmodium falciparum* FabZ (*PfFabZ*).<sup>24</sup> Recently, we discovered two synthetic compounds (**1** and **2**, Figure 1) as inhibitors of *H. pylori* FabZ (*HpFabZ*) with IC<sub>50</sub> values of 39.8  $\pm$  0.35  $\mu$ M

<sup>†</sup> PDB ID codes: 2GLL, 3DOY, 3DOZ, 3DP0, 3DP1, 3DP2, and 3DP3.

\* To whom correspondence should be addressed (X.S.) Phone: +86-21-50806918. Fax: +86-21-50807088. E-mail: xshen@mail.shnc.ac.cn. (H.J.) Phone: +86-21-50805873. Fax: +86-21-50807088. E-mail: hljiang@mail.shnc.ac.cn. (H.L.) Phone: +86-21-50807042. Fax: +86-21-50807088. E-mail: hliu@mail.shnc.ac.cn.

<sup>‡</sup> Authors equally contributed to this work.

<sup>§</sup> Center for Drug Discovery and Design, State Key Laboratory of Drug Research, Shanghai Institute of Materia Medica, Chinese Academy of Sciences.

<sup>||</sup> School of Pharmacy, East China University of Science and Technology.

<sup>a</sup> Abbreviations: FabZ,  $\beta$ -hydroxyacyl-acyl carrier protein dehydratase; *Hp*, *Helicobacter pylori* or *H. pylori*; FAS-I, type I fatty acid biosynthesis; FabD, malonyl-CoA:ACP transacylase; FabH,  $\beta$ -ketoacyl-acyl carrier protein synthase III; FabF,  $\beta$ -ketoacyl-acyl carrier protein synthase II; FabB,  $\beta$ -ketoacyl-acyl carrier protein synthase I; FabI, enoyl-acyl carrier protein reductase; FabA,  $\beta$ -hydroxyacyl-acyl carrier protein dehydratase; FabG,  $\beta$ -ketoacyl-ACP reductase I; ACP, the acyl carrier protein; CoA, acetyl coenzyme A; *PfFabZ*, *Plasmodium falciparum* FabZ.

and  $47.6 \pm 0.29 \mu\text{M}$ , respectively.<sup>25</sup> In addition, we also determined the X-ray crystal structures of *HpFabZ* in complex with these inhibitors, which demonstrated the inhibitory mechanism of FabZ for the first time.<sup>25</sup> In this study, on the basis of the structures and activities of compounds **1** and **2**, and their interactive models with *HpFabZ* as well, we identified several small compounds that inhibit *HpFabZ* activity with  $\text{IC}_{50}$  values of  $0.86\text{--}42.7 \mu\text{M}$  by employing a comprehensive approach integrating structure-based design, focused-library design, virtual screening, chemical synthesis, and bioassay.

We approached anti-*H. pylori* therapeutic development employing structure-based design to identify small organic compounds as lead candidates. In the first phase of this study, we designed and synthesized two series of derivatives of compounds **1** and **2** according to the structural models of these inhibitors binding to *HpFabZ*. Five compounds showed high inhibition activities with  $\text{IC}_{50}$  values less than  $2 \mu\text{M}$ , nearly 28 times more potent than the initial starting hits **1** and **2**. Afterward, the crystal structures of the complexes of six compounds with the *HpFabZ* were determined. In the second phase, we adopted a strategy integrating focused combinatorial library design, virtual screening, chemical synthesis, and bioassay to identify more potent inhibitors based on the result of the first phase. Using the fragments taken from the *HpFabZ* inhibitors identified in the first phase, a focused combinatorial library containing 280 molecules was designed by employing the LD1.0 program<sup>26</sup> on the basis of the crystal structures of the inhibitor-*HpFabZ* complexes. By using docking-based virtual screening targeting the binding site of *HpFabZ*, 12 compounds (**5a–l**) were selected for synthesis and bioassay. Eight compounds showed *HpFabZ* enzymatic inhibition activities with  $\text{IC}_{50}$  values of  $0.86\text{--}42.7 \mu\text{M}$ . The inhibitory activity of the most potent compound increased 46 times more than that of the original compounds. All the inhibitors discovered in this study showed weak antibacterial activity, overcoming the shortcomings of the original inhibitors (compounds **1** and **2**) due to improving the druglikeness of the designed compounds. The high hit rate and the high potency of the new *HpFabZ* inhibitors demonstrated the efficiency of the discovery strategy used in this study. In addition, the chemical entities reported in this study could be leading factors contributing to the discovery of new therapies against the FAS-II pathway.

## 2. Materials and Methods

**2.1. Discovery Strategy.** On the basis of our previously discovered *HpFabZ* inhibitors (compounds **1** and **2**) and the crystal structures of the inhibitor-*HpFabZ* complexes, we started to design the new generation *HpFabZ* inhibitors to increase the enzymatic and antibacterial activities. The flowchart of the discovery strategy and procedure is outlined in Figure 2. In general, the inhibitor-designing process was conducted in a two-phase manner. During the phase I design, a series of derivatives of compounds **1** and **2** were designed and synthesized by a structure-based drug design approach according to the binding models of compounds **1** and **2** with *HpFabZ*. Several potent inhibitors were selected via an enzymatic activity assay, and the crystal structures of the complexes of the most potent inhibitors with *HpFabZ* were determined, which was the starting point for the phase II design. During the phase II design, a focused library containing 280 compounds was designed by using the fragments isolated from the inhibitors obtained in the phase I design as building blocks according to the inhibitor-*HpFabZ* binding models derived from the crystal structures. The structures in the focused library were docked

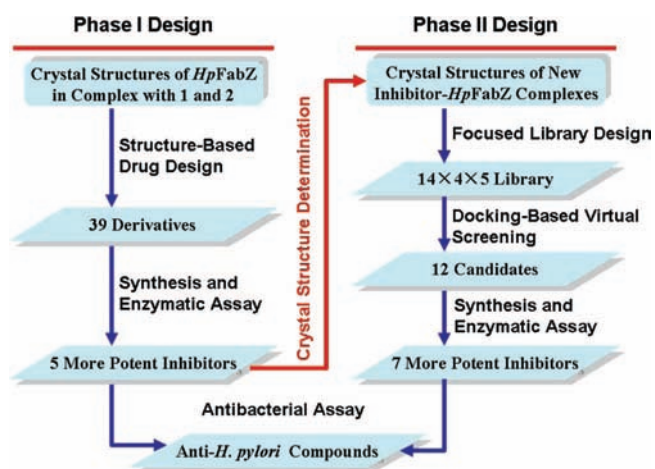


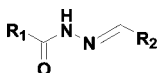
Figure 2. Discovery strategy and experimental flowchart in this study.

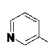
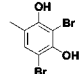
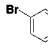
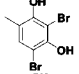
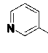
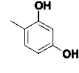
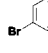
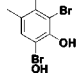
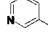
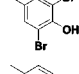
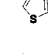
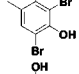
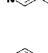
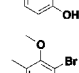

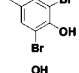

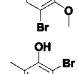

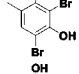

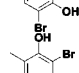
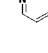
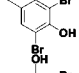

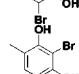

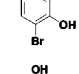
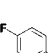
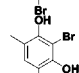

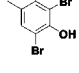
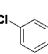
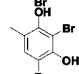
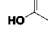
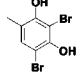
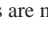
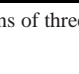
back into the binding pockets of *HpFabZ* and were scored by virtual screening functions to select candidates for further synthesis and bioassay. Several new inhibitors were discovered in this phase of the design. Finally, the bacterial growth inhibitory activities of all the obtained *HpFabZ* inhibitors were assessed. The detailed experimental procedures of each step are described in the following sections.

**2.1.1. Phase I Design.** On the basis of the structural feature and their interaction models with *HpFabZ* of compounds **1** and **2**, 39 new analogues (**3a–r** and **4a–u**, Tables 1 and 2) were designed and synthesized in the first phase. Keeping the pyridine ring of compound **1**, we obtained compounds **3a–d** by the removal of the hydroxyl group or bromide or by introducing methoxyl groups to the phenyl ring. Keeping the 2,4-dihydroxy-3,5-dibromo phenyl ring and replacing the pyridine ring with the phenyl ring, substituted phenyl ring, methyl, naphthalene ring, or various heterocycles, we obtained compounds **3e–r**. On the basis of the structural features of compound **2**, we designed compounds **4a–u** (Table 2). By changing the substituent groups of the substitutional phenyl ring  $\text{R}_3$  of compound **2**, we got compounds **4a–c**. Compounds **4d–r** were obtained by introducing various electronic, hydrophobic groups to the *ortho*-, *meta*-, or *para*- position of the unsubstituted phenyl ring  $\text{R}_4$  of compound **2** or displacing the  $\text{R}_4$  group with the naphthalin ring. Compounds **4s–u** were obtained by displacing the methoxy group with three different amino groups.

**2.1.2. Phase II Design.** Before phase II design, the X-ray crystal structures of *HpFabZ* in complex with the inhibitors produced from phase I design were determined, which provide inhibitor-enzyme interaction models for further inhibitor design. A focused library was designed using the structural fragments isolated by the above discovered inhibitors according to the inhibitor-enzyme interaction models. The LD1.0 program<sup>26,27</sup> was used during the focused library design. The inhibitor-enzyme interaction models indicate that the *HpFabZ* inhibitors can be divided into three parts (Figure 3A): part A is located in the large pocket (site A), part B interacts with the small pocket of *HpFabZ* (site B), and part L is a linker between A and B, interacting with the “saddle” pocket between sites A and B, with a length of  $5\text{--}6 \text{ \AA}$  (Figure 3A, middle image). From fragments of *HpFabZ* inhibitors discovered above and previously,<sup>25,28</sup> the LD1.0 program optimized 14 fragments for part A, 5 fragments for part B, and 4 linkers for part L. The chemical structures of the fragments are shown in Figure 4. Then LD1.0 connected these fragments together according to the structure

**Table 1.** Chemical Structures, *HpFabZ* Inhibitory Activities, and Antibacterial Activity of Compounds **1** and **3a–r**



| Compd     | R <sub>1</sub>  | R <sub>2</sub>  | % inhibition<br>at 50 μM | IC <sub>50</sub> <sup>a</sup> (μM) | MIC (μg/ml)    |                | Compd     | R <sub>1</sub>  | R <sub>2</sub>   | % inhibition<br>at 50 μM | IC <sub>50</sub> <sup>a</sup> (μM) | MIC (μg/ml)    |                |
|-----------|---|---|--------------------------|------------------------------------|----------------|----------------|-----------|---|--|--------------------------|------------------------------------|----------------|----------------|
|           |   |   |                          |                                    | SS1            | ATCC<br>43504  |           |   |  |                          |                                    | SS1            | ATCC<br>43504  |
| <b>1</b>  |    |    | 71.40                    | 39.8±0.35                          | -              | -              | <b>3j</b> |    |    | 94.20                    | 1.50±0.25                          | 100            | 100            |
| <b>3a</b> |    |    | 25.60                    | -                                  | -              | -              | <b>3k</b> |    |    | 96.00                    | 1.98±0.21                          | 100            | 100            |
| <b>3b</b> |    |    | 62.10                    | -                                  | -              | -              | <b>3l</b> |    |    | 72.00                    | -                                  | -              | -              |
| <b>3c</b> |    |    | 15.10                    | -                                  | -              | -              | <b>3m</b> |    |    | 92.60                    | 1.42±0.28                          | 50             | 100            |
| <b>3d</b> |    |    | 64.40                    | -                                  | -              | -              | <b>3n</b> |    |    | 81.40                    | 9.92±0.59                          | - <sup>b</sup> | - <sup>b</sup> |
| <b>3e</b> |    |    | 38.80                    | -                                  | -              | -              | <b>3o</b> |    |    | 36.40                    | -                                  | -              | -              |
| <b>3f</b> |    |    | 39.40                    | -                                  | -              | -              | <b>3p</b> |    |    | 15.20                    | -                                  | -              | -              |
| <b>3g</b> |   |   | 23.30                    | -                                  | -              | -              | <b>3q</b> |   |   | 74.40                    | 1.52±0.11                          | 50             | 100            |
| <b>3h</b> |  |  | 85.00                    | 6.43±1.36                          | - <sup>b</sup> | - <sup>b</sup> | <b>3r</b> |  |  | 50.00                    | -                                  | -              | -              |
| <b>3i</b> |  |  | 93.80                    | 1.52±0.19                          | >100           | >100           |           |   |  |                          |                                    |                |                |

<sup>a</sup> Values are means of three determinations and deviation from the mean is <10% of the mean value. <sup>b</sup> Due to poor solubility without antibacterial activity bioassay.

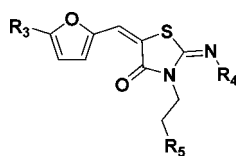
of *HpFabZ* binding site, producing a library containing 280 (14 × 4 × 5) molecules. All molecules in the designed library were ranked by the scoring functions of DOCK4.0, AutoDock4.0, and the druglikeness filter of LD1.0 (Figure S1 and Table S1 of the Supporting Information) and analyzed for relatively lower binding energy, favorable shape complementarity, and potential in forming hydrogen bonds with *HpFabZ*. In this way, 12 compounds (**5a–l**) were finally selected for synthesis and bioassay.

**2.2. Chemical Synthesis.** Compounds **3–5** were synthesized through the routes outlined in Schemes 1 and 2. Compounds **6** and **9** were brominated by Br<sub>2</sub> in 95% EtOH at room temperature, affording **7** and **10**, respectively.<sup>29</sup> Compound **7** was methylated by (CH<sub>3</sub>)<sub>2</sub>SO<sub>4</sub> in DMF in the presence of K<sub>2</sub>CO<sub>3</sub> at 100 °C.<sup>30</sup> Commercially available acid **11** was successfully converted to acid hydrazide **12** by a sequential esterification and hydrazinolysis. Then acid hydrazide **12** was condensed with **6**, **7**, **8**, **9**, and **10** in anhydrous EtOH at room temperature, giving the target compounds **1**, **3a–r**, and **5a–j**, respectively.<sup>31</sup>

Scheme 2 depicts the sequence of reactions that led to the preparation of compounds **2**, **4a–u**, and **5k–l**. Treatment of isothiocyanate **13** with amine **14** in toluene at room temperature quickly afforded thiourea **15a–q** and **5k** to produce good yields.<sup>32</sup> Thiourea **15a–q** were condensed with chloroacetic acid and sodium acetate anhydrous in anhydrous EtOH to produce **16a–q**. Commercially available substituted amines **17a–b** were esterified to afford esters **18a–b**. Compounds **18a–b** were

dissolved in hydrochloric acid, and diazotized by the addition of a sodium nitrite solution at 0 °C and then treated with 2-furfuraldehyde and cupric chloride to give **19a–b** as products.<sup>33</sup> In the same manner as the preparation of **19a–b**, **19c** was prepared from 4-chloro aniline and 2-furfuraldehyde. **19a–c** was condensed with **16a–q** in EtOH in the presence of piperidine and then hydrolyzed in THF in the presence of LiOH, affording the target compounds **2** and **4a–u**. Treatment of commercially available acid **20** with anilines **21** in the presence of pyridine produced amides **5l**. The details of the synthetic procedures and structural characterizations are described in the Experimental Section. The combustion analyses and the purities of all these compounds are listed in Tables S2 and S3 in the Supporting Information, respectively.

**2.3. Compound Screening. 2.3.1. Virtual Screening.** The binding potential between *HpFabZ* and molecules enumerated from the focused library were evaluated by the scoring module of LD1.0. Docking algorithm and scoring function of DOCK4.0<sup>34,35</sup> were adopted in the virtual screening. The scoring function of AutoDock4.0<sup>36</sup> was also used to rank the molecules to avoid the inaccuracy of one scoring function. The X-ray crystal structure of *HpFabZ* was used as a target for the virtual screening. Residues of *HpFabZ* around the binding site at a radius of 6.5 Å were isolated for constructing the grids of the docking screening. The resulting substructure included all residues of the binding pocket. During the docking simulation, Kollman-all-atom charges<sup>37</sup> were assigned to the protein atoms

**Table 2.** Chemical Structures of Compounds **2** and **4a–u** and Their *HpFabZ* Inhibitory Activities

| Compound  | R <sub>3</sub> | R <sub>4</sub> | R <sub>5</sub> | % inhibition at 50 μM | Compound  | R <sub>3</sub> | R <sub>4</sub> | R <sub>5</sub> | % inhibition at 50 μM |
|-----------|----------------|----------------|----------------|-----------------------|-----------|----------------|----------------|----------------|-----------------------|
| <b>2</b>  |                |                |                | 63.90                 | <b>4k</b> |                |                |                | NA                    |
| <b>4a</b> |                |                |                | NA                    | <b>4l</b> |                |                |                | NA                    |
| <b>4b</b> |                |                |                | NA                    | <b>4m</b> |                |                |                | 19.9                  |
| <b>4c</b> |                |                |                | NA                    | <b>4n</b> |                |                |                | NA                    |
| <b>4d</b> |                |                |                | NA                    | <b>4o</b> |                |                |                | 12.6                  |
| <b>4e</b> |                |                |                | 15.4                  | <b>4p</b> |                |                |                | NA                    |
| <b>4f</b> |                |                |                | NA                    | <b>4q</b> |                |                |                | NA                    |
| <b>4g</b> |                |                |                | NA                    | <b>4r</b> |                |                |                | 10.0                  |
| <b>4h</b> |                |                |                | 12.0                  | <b>4s</b> |                |                |                | NA                    |
| <b>4i</b> |                |                |                | NA                    | <b>4t</b> |                |                |                | NA                    |
| <b>4j</b> |                |                |                | 32.2                  | <b>4u</b> |                |                |                | NA                    |

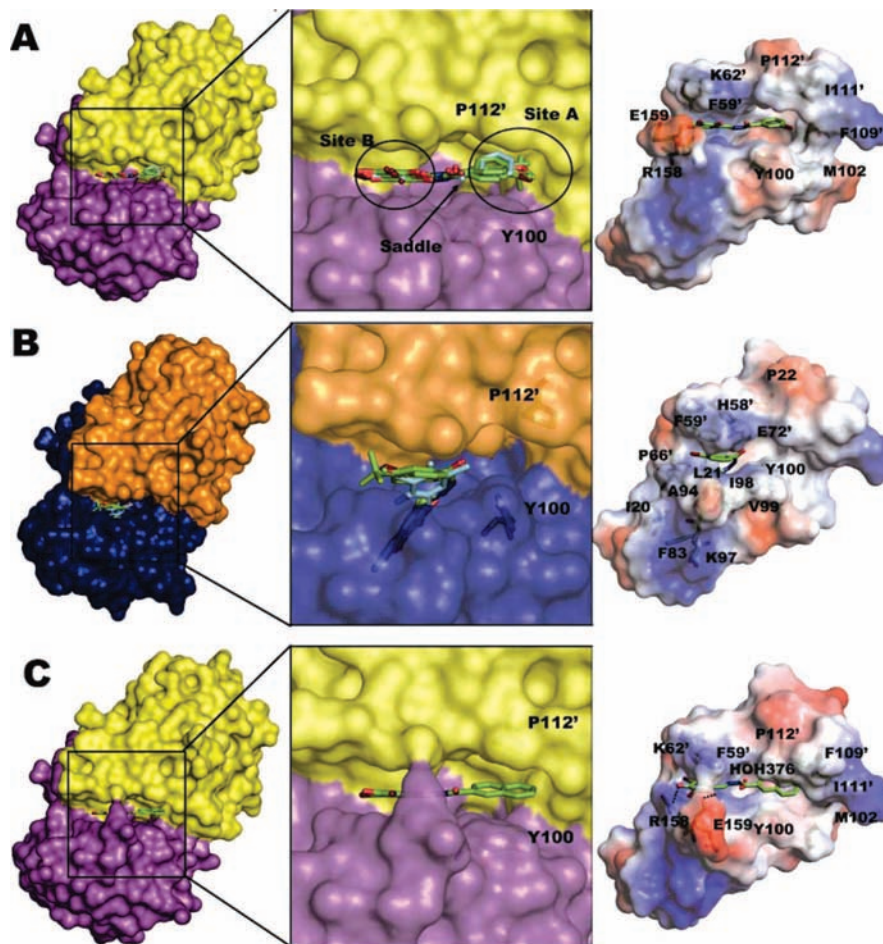
and Gasteiger–Marsili charges<sup>38</sup> were assigned to the ligand atoms in the library. Conformational flexibility of the molecules from the library was considered in the docking search.

The druglikeness of molecules from the combinatorial library was also evaluated by the druglikeness filter of LD1.0.<sup>26</sup> The druglikeness descriptor set encoded in LD1.0 is composed of the “Rule of Five” and the other three descriptors of the structural ratio.<sup>39,40</sup> For obtaining more information and understanding the synthetical alternation, we broadened the constraint of the molecular weight to 600. The range of evaluation on druglikeness is between 0 and 1, which stands for nondruglikeness and druglikeness, respectively.<sup>40</sup> All the parameters used in the LD1.0 were described in our previous paper.<sup>26</sup>

**2.3.2. Enzymatic Activity Assay.** The enzymatic inhibition assay of *HpFabZ* was monitored by the spectrophotometric method as described previously.<sup>21,25</sup> In brief, the activity of *HpFabZ* was measured by the detection of the decrease in absorbance at 260 nm for the conversion of crotonoyl-CoA to

$\beta$ -hydroxybutyryl-CoA. The compounds dissolved in 1% DMSO were incubated with the enzyme for 1 h before the assays were started. The 50% inhibitory concentration (IC<sub>50</sub>) of each inhibitor was estimated by fitting the inhibition data to a dose-dependent curve using a logistic derivative equation.<sup>41</sup>

**2.3.3. Antibacterial Assay.** The bacterial growth inhibition activity for the compounds was evaluated by using the paper discus method. Dimethyl sulfoxide and ampicillin paper were used as negative and positive controls respectively. The minimum inhibitory concentration (MIC) values were determined by the standard agar dilution method<sup>42</sup> using Columbia agar supplemented with 10% sheep blood containing 2-fold serial dilutions of agents. A bacterial suspension of *H. pylori* was made by swabbing and suspending the cells in sterile saline with a turbidity equivalent to a 2.0 McFarland standard. Compound-free Columbia agar media were used as controls. Inoculated plates were incubated at 37 °C under microaerobic conditions (85% N<sub>2</sub>, 10% CO<sub>2</sub>, and 5% O<sub>2</sub>) and examined after



**Figure 3.** Crystal structures of *HpFabZ* in complex with compounds **3i**, **3j**, **3k**, **3m**, **3n**, and **3q**. (A) Binding model A of compounds **3i–k**, **3n**, and **3q** in pocket A. The electrostatic surface of the *HpFabZ* active tunnel is generated by Pymol.<sup>51</sup> The binding sites of compounds (binding site A, saddle and site B) and the critical residues that interact with the compounds are shown. Oxygen, nitrogen, and sulfur atoms are colored red, blue, and orange, respectively. (B) Binding model B of compounds **3i–k**, **3n**, and **3q** in pocket B. (C) Binding model of compound **3m** in pocket A. The schematic picture is prepared by Pymol.<sup>51</sup>

3 days. The MIC was generally defined as the lowest concentration of antimicrobial agents that completely inhibits visible bacterial growth.

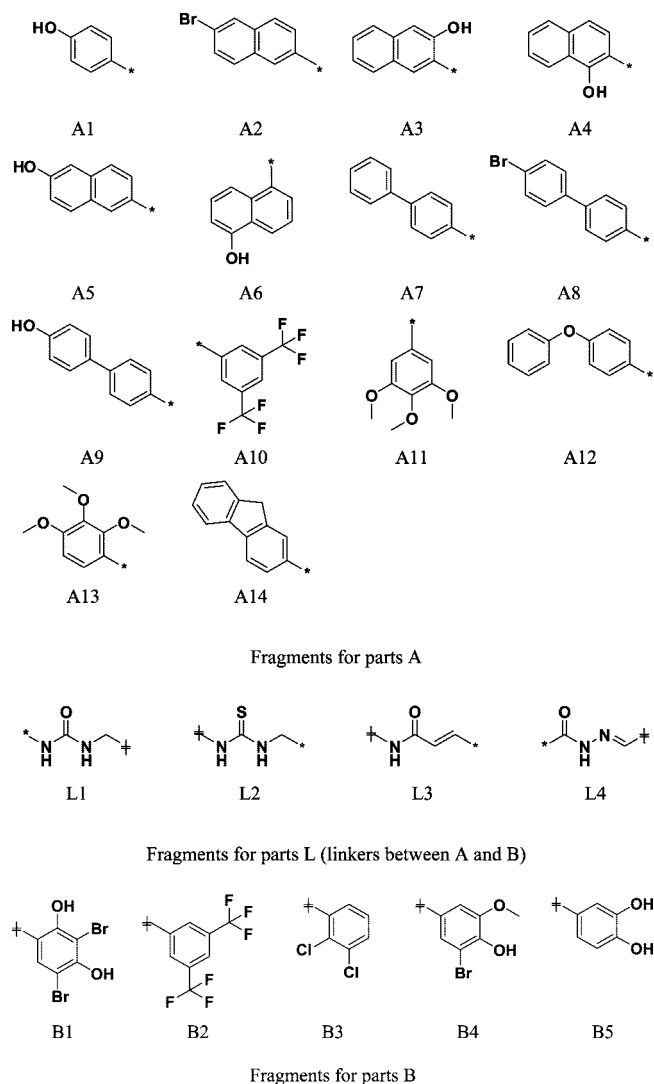
### 3. Results and Discussion

**3.1. Identification of Inhibitors by Phase I Design.** In our previous study,<sup>25</sup> we discovered two small molecular inhibitors of *HpFabZ* (compounds **1** and **2**) and determined the X-ray crystal structures of the inhibitor–enzyme complexes. This provided a solid foundation for designing more potent *HpFabZ* inhibitors. Compound **1** is composed of a pyridine ring and a 2,4-dihydroxy-3,5-dibromo phenyl ring linked by a formohydrazide moiety. The crystal structure revealed that two molecules of compound **1** bind to one hexamer of *HpFabZ* with two distinct interactive models: one molecule fits into the groove around the entrance (model A, Figure 5) and the other molecule lies at the active site of the tunnel (model B, Figure 5). Compound **2** is mainly composed of four rings: a phenyl ring at one end, a 2-chloro-benzoic acid moiety at the other end, and two heterocycles (a furan ring and a thiazolidinone substituted by a 2-methoxy-ethyl chain) in the middle. The crystal structure illustrated that compound **2** binds to monomer B of *HpFabZ* with a binding model similar to model A of compound **1**. In model A, the two aromatic ends of either compound **1** or **2** are sandwiched between the two “lips” of the *HpFabZ* entrance via hydrophobic interactions. Hence, during

phase I design, we modify the two aromatic ends of compounds **1** and **2** to enhance the hydrophobic interactions with the enzyme, producing 39 compounds (designated as series **3** and **4**).

The chemical structures of the 39 designed compounds (**3a–r** and **4a–u**) are shown in Tables 1 and 2. These compounds were synthesized through the routes outlined in Schemes 1 and 2, and the details of the synthetic procedures and structural characterizations are described in the Experimental Section. The primary inhibitory activities of these compounds at 50  $\mu\text{M}$  against *HpFabZ* were determined, and the results are also listed in Tables 1 and 2. Bioassay detail is described in the Experimental Section.

The primary data indicate that seven compounds (**3h–k**, **3m**, **3n**, and **3q**) are more active than the leading hit (compound **1**) (Table 1). Encouraged by this result, we determined the quantitative inhibition activities ( $\text{IC}_{50}$  values) for seven compounds. The results are also listed in Table 1. As  $\text{IC}_{50}$  values indicated, the inhibitory activities of these seven inhibitors increased about 4–28 times in comparison with that of compound **1**. Structure–activity relationship results indicated that removal of the bromine substituents of the phenyl ring (**3a–3c**) or replacement of the hydroxyl group with methoxyl (**3d**) decreases the inhibitory activities of compounds. The inhibitory activities of compounds (**3e**, **3f**, **3p**, and **3r**) obtained by replacing the pyridine ring of **1**, respectively, with phenyl



**Figure 4.** Building blocks for focused library generation. Fragments for parts A, B, and L were isolated for our previously discovered *HpFabZ* inhibitors. The symbols \* and  $\oplus$  represent the sites where fragments connect each other to form a complete structure.

ring, furan ring, methyl, and 4-hydroxy benzyl decreased. While compounds produced by replacing the pyridine ring of **1** with more hydrophobic groups such as halogen (F, Cl, and Br) substituted phenyl rings (**3g–k**), a naphthalene ring (**3m**) and a methoxy substituted phenyl ring (**3n**) show more potent inhibitory activities than that of compound **1**. Slight improvement in inhibitory activities were observed when the pyridine ring of **1** was displaced by a thiophene ring (**3l**) and a *tert*-butyl substituted phenyl ring (**3q**). When the position of the N-atom of the pyridine ring is changed (**3o**), tremendous decrease of inhibitory activities was observed.

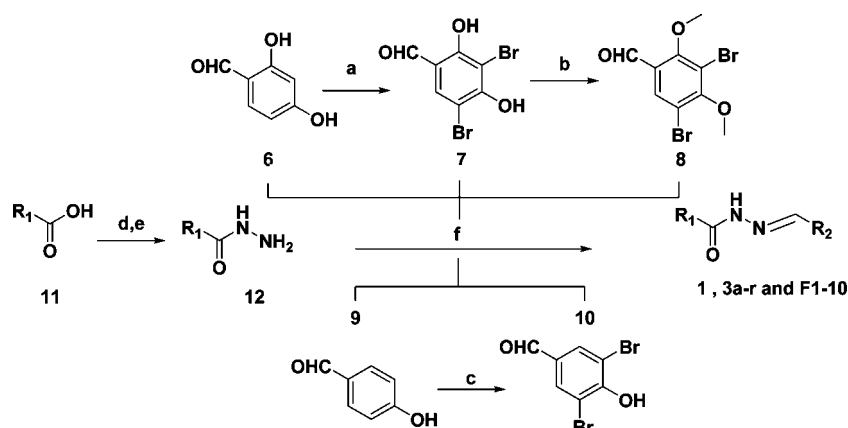
Table 2 lists the chemical structures and inhibitory data of compound **2** and its derivatives **4a–u**. Unfortunately, no potent active compounds have been discovered by the modification of compound **2**, most of derivatives were proven to have completely lost the inhibitory activities. Accordingly, in the following X-ray crystallography study and new inhibitor design, we only focused on the analogues of compound **1**.

**3.2. Binding Models of the Inhibitors to *HpFabZ* Detected by X-ray Crystallography.** To obtain more information for further inhibitor design and to investigate the potential inhibition mechanism, we determined the three-dimensional (3D) structures for the complexes of *HpFabZ* with the seven most

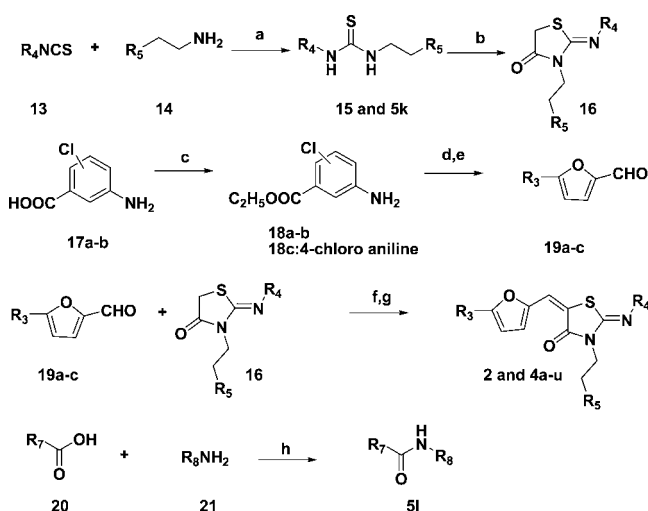
potent inhibitors (**3h–k**, **3m**, **3n**, and **3q**) using X-ray crystallography. Except inhibitor **3h**, all other six compounds soaked into the binding sites of *HpFabZ*. The structural models are shown in Figure 3 and Figure S2 in the Supporting Information. The coordinates and structural factors of these crystal structures have been deposited in the Protein Data Bank (PDB codes are 3DOY, 3DOZ, 3DP0, 3DP1, 3DP2, and 3DP3, respectively). The binding models of these compounds with *HpFabZ* are shown in Figure 3. The crystal structures were determined by molecular replacement (MR) to resolutions of 2.3–2.5 Å. The final structures of inhibitor–*HpFabZ* are well ordered, and the electron densities for all residues with the exception of the N-terminus (residues 1–10) are clearly interpretable. The statistics of the diffraction data and structure refinement are listed in Tables S4 and S5 in the Supporting Information. The overall structure of *HpFabZ* in the complexes is similar to that of the native *HpFabZ* (PDB code is 2GLL),<sup>25</sup> displaying a classic “trimer of dimers” organization. Each *HpFabZ* dimer forms two substrate-binding tunnels with catalytic sites on the interface, which are ~20 Å away from each other (Figure S2 in the Supporting Information).

Except compound **3m**, five other inhibitors bind to *HpFabZ* in a similar way to compound **1**.<sup>25</sup> For **3i–k**, **3n**, and **3q**, two molecules of each compound bind to one hexamer of *HpFabZ* with two distinct interaction models: one molecule fits into the groove around the entrance with an extended conformation (Figure 3A) (designated as model A hereinafter); the other molecule lies at the active site of the tunnel with a folded conformation (Figure 3B) (called model B below). For model A, Tyr100 and Phe83 adopt open and closed conformations, respectively, thus the R<sub>1</sub> substituent (see Table 1) of each compound is located between the phenol ring of Tyr100 and the pyrrolidine ring of Pro112', forming a sandwich structure, and the R<sub>2</sub> substituent at the other end of the inhibitor binds into a pocket composed of Arg158, Glu159, Phe59', and Lys62' through hydrophobic interactions, particularly, the aromatic ring of R<sub>2</sub> substituent form a  $\pi\cdots\pi$  stacking interaction with the side chain of Phe69', and cation $\cdots\pi$  interactions with the positively charged side chains of Lys62' and Arg158 (Figure 3A). For model B, Tyr100 adopted a closed conformation and Phe83 adopted an open conformation and the whole molecules of the inhibitors entered into the middle of the tunnel, located near the active site of *HpFabZ* (His58 and Glu72'). However, the orientation of the designed inhibitors inside the tunnel of enzyme is opposite to that of compound **1**: the R<sub>1</sub> substituent is sandwiched between Ile98 and Phe59', while the R<sub>2</sub> substituent moves deeply to the catalytic site of the tunnel, contacting with Ile20, Leu21, Pro22, Phe83, Ala94, Lys97, and Val99 via hydrophobic interactions (Figure 3B).

Different from the other five inhibitors, compound **3m** was observed to bind to *HpFabZ* only with model A. The reason is possibly that the steric hindrance caused by the bulky naphthalene prevents the inhibitor from entering further into the tunnel (Figure 3C). Also, compound **3m** fits well into the entrance of the tunnel with an extended conformation; however, the 2,4-dihydroxy-3,5-dibromo phenyl ring binds more tightly with the hydrophobic pocket lined by Arg158, Glu159, Phe59', and Lys62' so that two hydroxyl groups of **3m** form two strong hydrogen bonds (H-bonds), respectively, with the backbone carbonyl of Glu159 and the guanidinium group of Arg158. These additional H-bonds led **3m** to be equal or more active than other compounds although this compound can only bind to the enzyme with one model.

Scheme 1<sup>a</sup>

<sup>a</sup> Reagents and conditions: (a) Br<sub>2</sub>, 95% EtOH, 25 °C; (b) (CH<sub>3</sub>)<sub>2</sub>SO<sub>4</sub>, K<sub>2</sub>CO<sub>3</sub>, DMF, 100 °C; (c) Br<sub>2</sub>, 95% EtOH, 25 °C; (d) EtOH, H<sub>2</sub>SO<sub>4</sub>, reflux 4 h; (e) hydrazine hydrate (85%), EtOH, reflux 4–8 h; (f) EtOH, 25 °C.

Scheme 2<sup>a</sup>

<sup>a</sup> Reagents and conditions: (a) toluene, rt, 1–2 h; (b) ClCH<sub>2</sub>COOH, CH<sub>3</sub>COONa, EtOH, reflux, 12 h; (c) MeOH, H<sub>2</sub>SO<sub>4</sub>, reflux; (d) HCl, NaNO<sub>2</sub>, 0 °C; (e) CuCl<sub>2</sub>, 2-furaldehyde, rt, 4 h; (f) piperidine, ethanol, reflux, 12 h; (g) LiOH, MeOH, rt, 4 h; (h) pyridine, rt, 5 h.

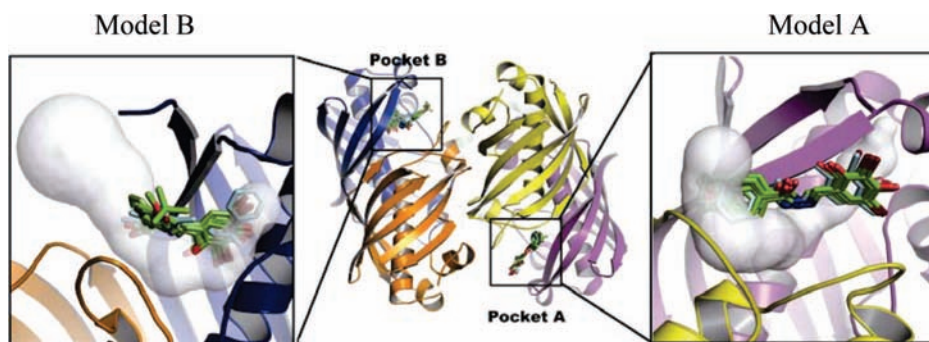
### 3.3. Identification of Inhibitors by the Phase II Design.

The two binding models of the phase I designed compounds with *HpFabZ* indicate that compounds with bulky substituents like compound **3m** still show high activities despite that only one binding model (model A) exists. This may be structurally attributed to that the 2,4-dihydroxy-3,5-dibromo phenyl ring binds more tightly with the hydrophobic pocket lined by Arg158, Glu159, Phe59', and Lys62' so that two hydroxyl groups of **3m** form two strong hydrogen bonds (H-bonds), respectively, with the backbone carbonyl of Glu159 and the guanidinium group of Arg158. Thus, in the phase II compound design, a focused library was designed only according to model A (Figure 3A). Model A clearly illustrates that the inhibitors discovered through the phase I design could be divided into three parts (Figure 3A): part A interacts with the large pocket of *HpFabZ* composed of Tyr100, Met102, Phe109', Ile111', and Pro112' (site A); part B resides in the small pocket lined by Lys62', Arg158, Glu159, Phe59', and Pro22 (site B); and part L is a linker between A and B, interacting with the "saddle" pocket between sites A and B with a length of 5–6 Å. According to the structural diversity of the previously discovered inhibitors, we selected 14 fragments for part A, five fragments for part B, and four linkers for part L (Figure 4). Combining these fragments

together, a 14 × 4 × 5 focused library was obtained by using LD1.0.<sup>26</sup> Targeting the crystal structure of *HpFabZ*, the focused library was screened by using the scoring function of DOCK4.0<sup>34,35</sup> that has been encoded in LD1.0. The interaction energies of these 280 molecules to *HpFabZ* calculated by the DOCK4.0 function range from −47.68 to −22.57 kcal/mol (Figure S1 and Table S1 in the Supporting Information). However, docking programs and scoring functions have a tendency to generate a significant number of false positives.<sup>43</sup> To reduce the number of false positives in compound selection, the binding poses of these 280 molecules with *HpFabZ* were redocked using AutoDock4.0,<sup>36</sup> which has a better ability to optimize binding poses as well as predict binding energy.<sup>44</sup> AutoDock4.0 calculation indicates that the binding free energies of the compounds to *HpFabZ* range from −10.16 to −5.96 kcal/mol (Table S1 and Figure S1 in the Supporting Information). Considering these two scoring results, structural diversity, druglikeness, and synthetic feasibility, 12 compounds (**5a–l**) were selected and synthesized for actual biological testing and their chemical structures are shown in Table 3.

The primary inhibition activities of compounds **5a–l** against *HpFabZ* at 10 μM were measured. The results are also listed in Table 3. Of the 12 compounds, eight showed enhanced inhibition activities against *HpFabZ* at 10 μM. Thus, the IC<sub>50</sub> values of these eight compounds were also determined (Table 3) and the IC<sub>50</sub> values of five compounds (**5c**, **5f**, **5g**, **5h**, and **5j**) were discovered less than 4 μM. The IC<sub>50</sub> value of compound **5h** (0.86 ± 0.01 μM) was 46 times higher than that of starting compound **1** (IC<sub>50</sub> = 39.8 ± 0.35 μM). The focused library broadened the diversity of substituents R<sub>1</sub> and R<sub>2</sub> and the linkers between them. The result demonstrated that hydroxyl substituted naphthalene, 2,4-dihydroxy-3,5-dibromo phenyl ring and methyleneformohydrazide seem to be the optimized fragments for R<sub>1</sub>, R<sub>2</sub>, and linker.

**3.4. Antibacterial Activity.** Fifteen compounds (**3h–k**, **3m–n**, **3q**, **5b–d**, and **5f–j**) were shown to be inhibitors of *HpFabZ* through two cycles design. Their antibacterial activities were tested against the *H. pylori* strains SS1 and ATCC4 using the minimal inhibitory concentrations (MIC) approach. The results are listed in Tables 1 and 3. Twelve compounds showed weak antibacterial properties, with MIC values of 50–100 μg/mL. Because of poor solubility, we did not obtain the MIC values of compounds **3h** and **3n**. Compounds **3i** and **5b** are inactive in inhibiting the growth of *H. pylori* strain even at a concentration of >100 μg/mL. Among the compounds, **3m**, **3q**,



**Figure 5.** Schematic picture of the superposition of *HpFabZ*-compounds complex. Two molecules of each compound (except compound **3m**) bind to one hexamer of *HpFabZ* with two distinct interaction models. *HpFabZ* dimer A/B, C/D, compound **1**, compounds **3i**, **3j**, **3k**, **3m**, **3n**, and **3q** are colored yellow/magenta, blue/orange, cyan, and green, respectively. The active-site cavities are produced with the program MOLE<sup>52</sup> and shown in dark-gray surface representations.

**Table 3.** Chemical Structures, *HpFabZ* Inhibitory Activities and Antibacterial Activity of The 12 Compounds Selected From The Focused Library Using Virtual Screening

| Compd        | Structure | % inhibition<br>at 10 $\mu$ M | IC <sub>50</sub> <sup>a</sup> ( $\mu$ M) | MIC ( $\mu$ g/ml) |               |
|--------------|-----------|-------------------------------|--|-------------------|---------------|
|              |           |                               |  | SS1               | ATCC<br>43504 |
| <b>5a-5j</b> |           |                               |  |                   |               |
| <b>5a</b>    |           | 16.0%                         | -  | -                 | -             |
| <b>5b</b>    |           | 13.0%                         | 42.7 $\pm$ 2.87                          | >100              | >100          |
| <b>5c</b>    |           | 82.0%                         | 2.13 $\pm$ 0.08                          | 100               | 50            |
| <b>5d</b>    |           | 47.0%                         | 12.8 $\pm$ 0.19                          | No                | No            |
| <b>5e</b>    |           | 50.0%                         | -  | -                 | -             |
| <b>5f</b>    |           | 81.0%                         | 3.75 $\pm$ 0.72                          | 100               | 50            |
| <b>5g</b>    |           | 87.0%                         | 1.97 $\pm$ 0.31                          | 100               | 100           |
| <b>5h</b>    |           | 92.0%                         | 0.86 $\pm$ 0.01                          | 100               | 100           |
| <b>5i</b>    |           | 65.0%                         | 8.77 $\pm$ 0.25                          | 100               | 100           |
| <b>5j</b>    |           | 86.0%                         | 3.55 $\pm$ 0.28                          | 50                | 100           |
| <b>5k</b>    |           | 7.0%                          | -  | -                 | -             |
| <b>5l</b>    |           | 4.0%                          | -  | -                 | -             |

<sup>a</sup> Values are the means of three determinations and deviation from the mean is <10% of the mean value.

**5c**, **5f**, and **5j** displays encouraging antibacterial activity against one strain (SS1 or ATCC4) compared with compounds **1** and **2** without any antibacterial activity. Although the antibacterial activities of the compounds that were determined are not so

high in comparison with existing antibiotics, they provide leading factors contributing to the discovery of new therapies against the FAS-II pathway. Although the most potent inhibitor (compound **5h**) discovered in this study is structurally similar



to the patented antibacterial<sup>45</sup> or antimetazoan parasite compounds,<sup>46</sup> it is purely incidental. Nevertheless, this further illustrates that our discovery strategy is reasonable because the design procedure converged some of the *HpFabZ* inhibitors into similar structures of existing antibacterial compounds. In addition, the molecular targets of the patented antibacterial compounds are unknown, our study accidentally found that FabZ may be one of the targets of these compounds. Of note, this study only implied that *HpFabZ* is a target of the antibacterial compounds similar to **5h**. The target specificity of these compounds or whether their antibacterial activity is associated with other target needs to be further explored.

**3.5. Structure–Activity Relationship (SAR).** Bioassay indicates that, of the 12 binders, eight compounds (**5b–d** and **5f–j**) showed strong *HpFabZ* inhibitory activity with IC<sub>50</sub> values of 0.86–42.7 μM in Table 3 and the activity of the most potent one **5h** (0.86 μM) increased 46 times. Structurally, compounds **5a–j** have similar chemical scaffolds with the B1 fragment (Figure 4), indicating that B1 is the most optimized fragment for part B. Fragments for part A are structurally more diverse than fragments for part B; fragments A2–5, A7–10, and A14 are the building blocks of part A for the *HpFabZ* inhibitors. Observing the crystal structures, the linker is with a length of 5–6 Å, which can involve 3–4 atoms and is relatively rigid in a way that reduces the entropy loss when fitting into the steric restraint binding groove. Considering the length and rigidity of saddle and synthetic feasibility, the diversity of candidate linkers is constrained. According to bioisostere replacement, four representative linkers (L1–L4) were finally selected with similar length and rigidity in the focused library design. The results illustrated that compounds with moderate or potent *HpFabZ* activity contain the L4 regiment as the linker and indicated that L4 is the most favorable fragment for the linker between parts A and B. Accordingly, as the *HpFabZ* inhibitors, the building blocks for parts B and L are fixed at fragments B1 and L4 and the fragment for part A is a little bit flexible.

The reason underlying the structure–activity relationship of compounds **3** and **5** can be addressed from the X-ray crystal structures of *HpFabZ* in complex with **3i–k**, **3m**, **3n**, and **3q** (Figure 3). In model A, inhibitors bind to the entrance of *HpFabZ* tunnel: the substituted phenyl ring of compound **3** (except **3m**) is located between the phenol ring of Tyr100 and the pyrrolidine ring of Pro112', forming a sandwich structure. The hydrophobic interactions between the phenyl ring of inhibitors and residues Phe109', Ile111', and Met102 stabilized the inhibitors in the right place, and the 2,4-dihydroxy-3,5-dibromo phenyl ring at the other end of compound **1** binds with a pocket formed by Arg158, Glu159, Phe59', and Lys62' through hydrophobic interactions. Extraordinarily, the aromatic ring of R<sub>2</sub> substituent is involved in a π····π stacking interaction with the side chain of Phe59' in addition to cation–π interactions with the positively charged side chains of Lys62' and Arg158. In model B, compound **3** (except **3m**) entered into the middle of the tunnel, located near the active site of *HpFabZ* (His58 and Glu72'): the 2,4-dihydroxy-3,5-dibromo phenyl ring almost accessed the exit of the tunnel, contacting with Ile20, Leu21, Pro22, Phe83, Ala94, Lys97, and Val99 via hydrophobic interactions while the substituted phenyl is sandwiched between Ile98 and Phe59'. Different from the other five inhibitors, compound **3m** was observed to bind to *HpFabZ* only with model A. It exclusively adopted an extended linear conformation with good shape complementarity with the binding tunnel a little differently. Because of steric hindrance imposed by the bulky naphthalene ring of the inhibitor, the 2,4-

dihydroxy-3,5-dibromo phenyl ring binds more tightly with the hydrophobic pocket lined by Arg158, Glu159, Phe59', and Lys62' so that two hydroxyl groups of **3m** form two strong hydrogen bonds (H-bonds), respectively, with the backbone carbonyl of Glu159 and the guanidinium group of Arg158. The binding models of compound **3i–k**, **3m**, **3n**, and **3q** with *HpFabZ* clearly illustrated that structural modifications that increase the hydrophobicities of R<sub>1</sub> and R<sub>2</sub> may increase the inhibition activities due to enhancement of the binding affinity (Tables 2 and 3). Compounds with a large hydrophobic group (naphthalene ring or 9H-fluorene ring) possess the potent inhibitory activity due to forming two strong hydrogen bonds (H-bonds), respectively, with the backbone carbonyl of Glu159 and the guanidinium group of Arg158. The additional hydrogen bond play vital roles for these compounds binding to the *HpFabZ*, and this may be an important reason that these compounds could potentially inhibit *HpFabZ*. However, no further activity improvements were observed with even bulkier fragments (**5b**, **5e**, **5k**, and **5l**) than the substituent naphthalene; this probably contributed to the size limit of the pocket (site A in Figure 3).

#### 4. Conclusions

The discovery of *HpFabZ* inhibitors is now of special interest in the treatment of gastric diseases. In the present study, a series of hydrazine derivatives and a series of novel thiazolidone derivatives were designed, synthesized based on the screening hits **1** and **2**. All the compounds were evaluated by the cell-based assay for their inhibitory activities against *HpFabZ*. Six compounds (**3i**, **3j**, **3k**, **3m**, and **3q**) for concentration–response studies showed prominent inhibitory activities, five compounds with IC<sub>50</sub> values less than 2 μM, which is nearly 25 times more potent than the initial compound **1**. To discover novel entries of *HpFabZ* inhibitors with more potent activities, on the basis of the chemical structures of the *HpFabZ* inhibitors we discovered previously and the modes of binding to *HpFabZ* in the crystal of the complexes of small molecules with the *HpFabZ*, a focused library has been designed by using the combinatorial library design program LD1.0.<sup>26</sup> Through virtual screening and druglike analysis, 12 compounds were selected from the focused library for chemical synthesis and bioassay. Remarkably, eight compounds among the 12 molecules show *HpFabZ* inhibitor activities, with IC<sub>50</sub> values ranging from 0.86 to 42.7 μM (Table 3). The hit rate for inhibitors is 66.7%. In comparison with the results in the phase I design, inhibitory activities of the active compounds designed in the phase II are moderately improved (Table 3). The crystallography study demonstrated that six compounds (**3i–k**, **3m–n**, and **3q**) bind to the binding pocket of *HpFabZ* in a similar way: part A fits into site A, part B is located in site B, and part L interacts with the saddle site of *HpFabZ*. The bioassay results indicate that the fragment combinations for potent *HpFabZ* inhibitors are A2–5, A7–10, and L4 in conjunction with B1. In addition, most of the active compounds discovered in this study are leading factors contributing to the discovery of new therapies against the FAS-II pathway, so the encouraging results in vitro activities may possess potential for the treatment of *H. pylori* infections based on new mechanisms.

#### 5. Experimental Section

**Chemistry.** The reagents (chemicals) were purchased from Lancaster, Acros, and Shanghai Chemical Reagent Company and used without further purification. Analytical thin-layer chromatography (TLC) was HSGF 254 (150–200 μm thickness, Yantai

Huiyou Company, China). Yields were not optimized. Melting points were measured in capillary tube on a SGW X-4 melting point apparatus without correction. Nuclear magnetic resonance (NMR) spectra were performed on a Bruker AMX-400 and AMX-300 NMR (IS as TMS). Chemical shifts were reported in parts per million (ppm,  $\delta$ ) downfield from tetramethylsilane. Proton coupling patterns were described as singlet (s), doublet (d), triplet (t), quartet (q), multiplet (m), and broad (br). Low- and high-resolution mass spectra (LRMS and HRMS) were given with electric, electrospray, and matrix-assisted laser desorption ionization (EI, ESI, and MALDI) produced by Finnigan MAT-95, LCQ-DECA spectrometer, and IonSpec 4.7 T, respectively. An Agilent 1100 Series HPLC with an Agilent Zorbax Eclipse XDB-C<sub>18</sub> (4.6 mm  $\times$  50 mm, 5  $\mu$ m) reversed phase column was used for analytical HPLC analyses. Preparative RP-HPLC was performed on an Agilent 1200 Series HPLC with an Agilent Zorbax Eclipse XDB-C<sub>18</sub> (9.4 mm  $\times$  250 mm, 5  $\mu$ m) column. The elution buffer was an A/B gradient, where A = H<sub>2</sub>O-0.1% TFA and B = CH<sub>3</sub>OH-0.1% TFA. Elemental analyses were performed on an Elementar Vario EL I analyzer.

**3,5-Dibromo-2,4-dihydroxy-benzaldehyde (7). Representative Procedure for 7 and 10.** To a stirred solution of **6** (2.76 g, 10 mmol) in EtOH (50 mL, 95%), Br<sub>2</sub> (2.5 mL, 50 mmol) was added dropwise at room temperature. Some pale-yellow solid appeared as Br<sub>2</sub> was added. Stirring was continued for 30 min. Thereafter, the suspension was poured into H<sub>2</sub>O (100 mL), filtered under suction, and the precipitate was washed with H<sub>2</sub>O for three times and recrystallized from EtOH/H<sub>2</sub>O (1:1 v/v) to give **7** as brown needles (3.49 g, 59.0%): mp 210–213 °C. <sup>1</sup>H NMR (300 MHz, CD<sub>3</sub>OD):  $\delta$  5.52 (s, 0.45H, OH), 7.39 (s, 0.45H, OH), 7.86 (s, 1H), 9.69 (s, 1H, -CH=O). EI-MS  $m/z$  294 (M<sup>+</sup>) 294 (100%). HRMS (EI)  $m/z$  calcd for C<sub>7</sub>H<sub>4</sub>Br<sub>2</sub>O<sub>3</sub> (M<sup>+</sup>) 293.8527, found 293.8527.

**3,5-Dibromo-4-hydroxy-benzaldehyde (10).** Melting point 181–183 °C. <sup>1</sup>H NMR (300 MHz, DMSO-*d*<sub>6</sub>):  $\delta$  8.08 (s, 2H), 9.80 (s, 1H, -CH=O). EI-MS  $m/z$  278 (M<sup>+</sup>) 278 (100%). HRMS (EI)  $m/z$  calcd for C<sub>7</sub>H<sub>4</sub>Br<sub>2</sub>O<sub>2</sub> (M<sup>+</sup>) 277.8578, found 277.8577.

**3,5-Dibromo-2,4-dimethoxy-benzaldehyde (8).** Compound **7** (148 mg, 0.5 mmol) was dissolved in DMF, and then K<sub>2</sub>CO<sub>3</sub> (700 mg, 5.0 mmol) and dimethyl sulfate (3.2 mL, 40.0 mmol) were added in sequence. The suspension was heated to 100 °C and stirred for 3 h until TLC indicated the completion of the reaction. After K<sub>2</sub>CO<sub>3</sub> was filtered off, the filtrate was poured into water and extracted with EtOAc for three times, and the combined organic layer were washed, dried over MgSO<sub>4</sub>, filtered, and concentrated to yield **8** (136 mg, 84.5%): mp 98–100 °C. <sup>1</sup>H NMR (300 MHz, CDCl<sub>3</sub>):  $\delta$  3.96 (s, 3H, -OCH<sub>3</sub>), 3.99 (s, 3H, -OCH<sub>3</sub>), 8.03 (s, 1H), 10.23 (s, 1H, -CH=O). EI-MS  $m/z$  321 (M<sup>+</sup>) 306 (100%). HRMS (EI)  $m/z$  calcd for C<sub>9</sub>H<sub>8</sub>Br<sub>2</sub>O<sub>3</sub> (M<sup>+</sup>) 321.8840, found 321.8840.

**1-Hydroxy-2-naphthoic Acid Hydrazide (12a). Representative Procedure for 12a–g.** 1-Hydroxy-2-naphthoic acid (190 mg, 1 mmol) was dissolved in EtOH, then H<sub>2</sub>SO<sub>4</sub> (catalysis) was added. The solution was refluxed for 8 h, and then the solvent was evaporated in vacuo. Water was added and the aqueous layer was back-extracted with ethyl acetate. The organic layer was washed with saturated sodium bicarbonate and brine. The combined organic extracts were dried over MgSO<sub>4</sub>, filtered through cotton, and concentrated in vacuo and then purified by chromatography with EtOAc/petroleum ether (1:20, v/v) to give ethyl 1-hydroxy-2-naphthoate as yellow–white oil. Yield 90.0%. <sup>1</sup>H NMR (CDCl<sub>3</sub>):  $\delta$  1.47 (t,  $J$  = 14.4 Hz, 3H), 3.71 (q, 2H), 7.29 (dd,  $J$  = 2.1 Hz and  $J$  = 2.1 Hz, 1H), 7.54 (t,  $J$  = 15.2 Hz, 1H), 7.59 (t,  $J$  = 16.6 Hz, 1H), 7.79 (d,  $J$  = 15.0 Hz, 2H), 8.44 (d,  $J$  = 9.3 Hz, 1H), 12.10 (s, 1H).

Ethyl 1-hydroxy-2-naphthoate was dissolved in hydrazine hydrate and heated to reflux for 8 h, and then the solvent was evaporated. Water was added, and the aqueous layer was back-extracted with ethyl acetate. The organic layer was washed with saturated sodium bicarbonate and brine. The combined organic extracts were dried over MgSO<sub>4</sub>, filtered through cotton, and concentrated in vacuo and then purified by chromatography with EtOAc/petroleum ether (1:15, v/v) to give **12a**. Yield 72.5%. <sup>1</sup>H NMR (DMSO-*d*<sub>6</sub>):  $\delta$  7.36

(d,  $J$  = 8.7 Hz, 1H), 7.53–7.66 (m, 2H), 7.85 (t,  $J$  = 15.6 Hz, 2H), 8.26 (dt,  $J$  = 1.9 Hz and  $J$  = 1.6 Hz, 1H).

**Biphenyl-4-carboxylic Acid Hydrazide (12b).** <sup>1</sup>H NMR (DMSO-*d*<sub>6</sub>):  $\delta$  7.38–7.43 (m, 1H), 7.49 (t,  $J$  = 15.0 Hz, 2H), 7.71–7.77 (m, 4H), 7.95 (d,  $J$  = 8.4 Hz, 2H).

**6-Bromo-2-naphthoic Acid Hydrazide (12c).** <sup>1</sup>H NMR (DMSO-*d*<sub>6</sub>):  $\delta$  7.71 (dd,  $J$  = 1.5 Hz and  $J$  = 1.5 Hz, 1H), 7.80–7.94 (m, 3H), 8.28 (d,  $J$  = 2.1 Hz, 1H), 8.45 (s, 1H).

**4-Phenoxy-benzoic Acid Hydrazide (12d).** <sup>1</sup>H NMR (DMSO-*d*<sub>6</sub>):  $\delta$  7.00–7.11 (m, 4H), 7.19–7.24 (m, 1H), 7.41–7.48 (m, 2H), 7.84–89 (m, 2H).

**6-Hydroxy-2-naphthoic Acid Hydrazide (12e).** <sup>1</sup>H NMR (DMSO-*d*<sub>6</sub>):  $\delta$  7.05–7.17 (m, 2H), 7.58–7.74 (m, 1H), 7.80–7.87 (m, 2H), 8.31 (s, 1H).

**9H-Fluorene-2-carboxylic Acid Hydrazide (12f).** <sup>1</sup>H NMR (DMSO-*d*<sub>6</sub>):  $\delta$  7.35–7.45 (m, 2H), 7.63 (d,  $J$  = 7.2 Hz, 1H), 7.88 (d,  $J$  = 8.4 Hz, 1H), 7.97 (d,  $J$  = 7.5 Hz, 2H), 8.06 (s, 1H). EI-MS  $m/z$  224 (M<sup>+</sup>) 193 (100%).

**4'-Hydroxy-biphenyl-4-carboxylic Acid Hydrazide (12g).** <sup>1</sup>H NMR (DMSO-*d*<sub>6</sub>):  $\delta$  6.83–6.90 (m, 2H), 7.56 (d,  $J$  = 8.1 Hz, 2H), 7.67 (d,  $J$  = 8.4 Hz, 2H), 7.87–7.94 (m, 2H).

**Nicotinic Acid (3,5-Dibromo-2,4-dihydroxy-benzylidene)-hydrazide (1). General Procedure for 1, 3a–r, and 5a–j.** The mixture of nicotinic acid hydrazide (137 mg, 1 mmol) and **7** (296 mg, 1 mmol) was dissolved in EtOH, and after a while, plenty of yellow precipitation appeared. The mixture was stirred at room temperature for 3 h. The precipitation was collected by filtration and washed with EtOH and purified using RP-HPLC to afford the final compound **1** (391 mg, 94.9%) as a yellow solid: mp 255–256 °C. <sup>1</sup>H NMR (300 MHz, DMSO-*d*<sub>6</sub>):  $\delta$  7.59 (dd,  $J$  = 5.1 and 7.8 Hz, 1H), 7.79 (s, 1H), 8.28 (dt,  $J$  = 7.8 and 1.8 Hz, 1H), 8.46 (s, 1H), 8.78 (dd,  $J$  = 5.1 and 1.2 Hz, 1H), 9.07 (d,  $J$  = 1.8 Hz, 1H). EI-MS  $m/z$  413 (M<sup>+</sup>) 106 (100%). HRMS (EI)  $m/z$  calcd for M<sup>+</sup>, 412.9011, found 412.8972. Anal. (C<sub>13</sub>H<sub>9</sub>Br<sub>2</sub>N<sub>3</sub>O<sub>3</sub>) calcd, C 37.62, H 2.19, N 10.12; found, C 37.99, H 2.20, N 10.03.

**Nicotinic Acid (2,4-Dihydroxy-benzylidene)-hydrazide (3a).** In the same manner as described in the preparation of **1**, **3a** was prepared from nicotinic acid hydrazide and 2,3-dihydroxy-benzaldehyde (**6**). Yield: 53.8%; mp 277–278 °C. <sup>1</sup>H NMR (300 MHz, DMSO-*d*<sub>6</sub>):  $\delta$  6.35 (m, 2H), 7.33 (d,  $J$  = 8.4 Hz, 1H), 7.57 (dd,  $J$  = 4.5 and 8.1 Hz, 1H), 8.24 (dt,  $J$  = 8.1 and 1.8 Hz, 1H), 8.49 (s, 1H),  $\delta$  8.75 (dd,  $J$  = 4.5 and 1.8 Hz, 1H), 9.04 (d,  $J$  = 1.5 Hz, 1H). EI-MS  $m/z$  257 (M<sup>+</sup>) 106 (100%). HRMS (EI)  $m/z$  calcd for M<sup>+</sup> 257.0080, found 257.0790. Anal. (C<sub>13</sub>H<sub>11</sub>N<sub>3</sub>O<sub>3</sub>) calcd C 60.70, H 4.31, N 16.33; found C 60.31, H 4.22, N 16.33.

**Nicotinic Acid (3,5-Dibromo-4-hydroxy-benzylidene)-hydrazide (3b).** In the same manner as described in the preparation of **1**, **3b** was prepared from nicotinic acid hydrazide and 3,5-dibromo-4-hydroxy-benzaldehyde (**10**). Yield: 59.6%; mp 275–276 °C. <sup>1</sup>H NMR (300 MHz, DMSO-*d*<sub>6</sub>):  $\delta$  7.56 (dd,  $J$  = 5.1 and 7.8 Hz, 1H), 7.94 (s, 2H), 8.24 (dt,  $J$  = 7.8 and 2.1 Hz, 1H), 8.28 (s, 1H),  $\delta$  8.75 (dd,  $J$  = 5.1 and 1.5 Hz, 1H), 9.03 (d,  $J$  = 1.8 Hz, 1H). EI-MS  $m/z$  397 (M<sup>+</sup>) 106 (100%). HRMS (EI)  $m/z$  calcd for M<sup>+</sup> 396.9061, found 396.9058. Anal. (C<sub>13</sub>H<sub>9</sub>Br<sub>2</sub>N<sub>3</sub>O<sub>3</sub>) calcd, C 39.13, H 2.27, N 10.53; found C 39.06, H 2.43, N 10.46.

**Nicotinic Acid (4-Hydroxy-benzylidene)-hydrazide (3c).** In the same manner as described in the preparation of **1**, **3c** was prepared from nicotinic acid hydrazide and 4-hydroxy-benzaldehyde (**9**). Yield: 64.2%; mp 247–249 °C. <sup>1</sup>H NMR (300 MHz, DMSO-*d*<sub>6</sub>):  $\delta$  6.84 (d,  $J$  = 8.4 Hz, 2H), 7.57 (m, 3H), 8.23 (dt,  $J$  = 7.8 and 2.1 Hz, 1H), 8.33 (s, 1H), 8.74 (dd,  $J$  = 4.8 and 1.5 Hz, 1H), 9.03 (d,  $J$  = 1.8 Hz, 1H). EI-MS  $m/z$  241 (M<sup>+</sup>) 106 (100%). HRMS (EI)  $m/z$  calcd for M<sup>+</sup> 241.0851, found 241.0860. Anal. (C<sub>13</sub>H<sub>11</sub>N<sub>3</sub>O<sub>2</sub>) calcd C 64.72, H 4.60, N 17.42; found C 64.49, H 4.48, N 17.39.

**Nicotinic Acid (3,5-Dibromo-2,4-dimethoxy-benzylidene)-hydrazide (3d).** In the same manner as described in the preparation of **1**, **3d** was prepared from nicotinic acid hydrazide and intermediate **8**, yielding, 61.8%; mp 186–189 °C. <sup>1</sup>H NMR (300 MHz, DMSO-*d*<sub>6</sub>):  $\delta$  3.85 (s, 6H), 7.59 (dd,  $J$  = 4.2 and 8.4 Hz, 1H), 8.13 (s, 1H), 8.26 (d,  $J$  = 8.4 Hz, 1H), 8.61 (s, 1H), 8.77 (d,  $J$  = 4.2 Hz, 1H), 9.08 (s, 1H). EI-MS  $m/z$  441 (M<sup>+</sup>) 321 (100%). HRMS

(EI)  $m/z$  calcd for  $M^+$  440.9324, found 440.9342. Anal. ( $C_{15}H_{13}Br_2N_3O_3$ ) calcd C 40.66, H 2.96, N 9.48; found C 40.41 H 2.79, N 9.11.

**Benzoic Acid (3,5-Dibromo-2,4-dihydroxy-benzylidene)-hydrazide (3e).** In the same manner as described in the preparation of **1**, **3e** was prepared from benzoic acid hydrazide and 3,5-dibromo-2,4-dihydroxy-benzaldehyde (**7**). Yield: 21.4%; mp 194–196 °C.  $^1H$  NMR (300 MHz, DMSO- $d_6$ ):  $\delta$  7.62 (m, 3H), 7.76 (s, 1H), 7.93 (d,  $J = 6.9$  Hz, 2H), 8.48 (s, 1H). EI-MS  $m/z$  412 ( $M^+$ ) 105 (100%). HRMS (EI)  $m/z$  calcd for  $M^+$  411.9058, found 411.9067. Anal. ( $C_{14}H_{10}Br_2N_2O_3$ ) calcd C 40.61, H 2.43, N 6.77; found C 40.84, 2.50, 6.70.

**Furan-2-carboxylic Acid (3,5-Dibromo-2,4-dihydroxy-benzylidene)-hydrazide (3f).** In the same manner as described in the preparation of **1**, **3f** was prepared from furan-2-carboxylic acid hydrazide and 3,5-dibromo-2,4-dihydroxy-benzaldehyde (**7**). Yield: 52.3%; mp 247–249 °C.  $^1H$  NMR (300 MHz, DMSO- $d_6$ ):  $\delta$  6.74 (dd,  $J = 2.1$  and 3.0 Hz, 1H), 7.34 (d,  $J = 3.0$  Hz, 1H), 7.74 (s, 1H), 7.98 (d,  $J = 2.1$  Hz, 1H), 8.47 (s, 1H). EI-MS  $m/z$  402 ( $M^+$ ) 95 (100%). HRMS (EI)  $m/z$  calcd for  $M^+$  401.8851, found 401.8848. Anal. ( $C_{12}H_8Br_2N_2O_4$ ) calcd, C 35.67, H 2.00, N 6.93; found C 35.92, H 2.10, N 6.82.

**3-Fluoro-benzoic Acid (3,5-Dibromo-2,4-dihydroxy-benzylidene)-hydrazide (3g).** In the same manner as described in the preparation of **1**, **3g** was prepared from 3-fluoro-benzoic acid hydrazide and 3,5-dibromo-2,4-dihydroxy-benzaldehyde (**7**). Yield: 45.4%; mp 247–249 °C.  $^1H$  NMR (300 MHz, DMSO- $d_6$ ):  $\delta$  7.62 (m, 5H), 8.46 (s, 1H). EI-MS  $m/z$  430 ( $M^+$ ) 123 (100%). HRMS (EI)  $m/z$  calcd for  $M^+$  429.8964, found 429.8961. Anal. ( $C_{14}H_9Br_2FN_2O_3$ ) calcd 38.92, H 2.10, N 6.48; found C 39.08, H 2.06, N 6.51.

**4-Fluoro-benzoic Acid (3,5-Dibromo-2,4-dihydroxy-benzylidene)-hydrazide (3h).** In the same manner as described in the preparation of **3c**, **3h** was prepared from 4-fluoro-benzoic acid hydrazide and 3,5-dibromo-2,4-dihydroxy-benzaldehyde (**7**). Yield: 48.6%; mp 232–234 °C.  $^1H$  NMR (300 MHz, DMSO- $d_6$ ):  $\delta$  7.26 (t,  $J = 8.7$  Hz, 2H), 7.52 (s, 1H), 7.96 (m, 2H), 8.33 (s, 1H). EI-MS  $m/z$  430 ( $M^+$ ) 123 (100%). HRMS (EI)  $m/z$  calcd for  $M^+$  429.8964, found 429.8955. Anal. ( $C_{14}H_9Br_2FN_2O_3$ ) calcd C 38.92, H 2.10, N 6.48; found C 39.26, H 2.40, N 6.55.

**4-Chloro-benzoic Acid (3,5-Dibromo-2,4-dihydroxy-benzylidene)-hydrazide (3i).** In the same manner as described in the preparation of **1**, **3i** was prepared from 4-chloro-benzoic acid hydrazide and 3,5-dibromo-2,4-dihydroxy-benzaldehyde (**7**). Yield: 16.2%; mp 208–211 °C.  $^1H$  NMR (300 MHz, DMSO- $d_6$ ):  $\delta$  7.64 (d,  $J = 8.4$  Hz, 2H), 7.78 (s, 1H), 7.96 (d,  $J = 8.4$  Hz, 2H), 8.46 (s, 1H). EI-MS  $m/z$  446 ( $M^+$ ) 139 (100%). HRMS (EI)  $m/z$  calcd for  $M^+$  445.8668, found 445.8653. Anal. ( $C_{14}H_9Br_2ClN_2O_3$ ) calcd C 37.49, H 2.02, N 6.25; found C 37.40, H 2.18, N 6.02.

**4-Bromo-benzoic Acid (3,5-Dibromo-2,4-dihydroxy-benzylidene)-hydrazide (3j).** In the same manner as described in the preparation of **1**, **3j** was prepared from 4-bromo-benzoic acid hydrazide and 3,5-dibromo-2,4-dihydroxy-benzaldehyde (**7**). Yield: 31.3%; mp 219–222 °C.  $^1H$  NMR (300 MHz, DMSO- $d_6$ ):  $\delta$  7.75 (m, 3H), 7.85 (d,  $J = 8.4$  Hz, 2H), 8.44 (s, 1H); EI-MS  $m/z$  490 ( $M^+$ ) 183 (100%). HRMS (EI)  $m/z$  calcd for  $M^+$ , 489.8163, found 489.8148. Anal. ( $C_{14}H_9Br_3N_2O_3$ ) calcd C 34.11, H 1.84, N 5.68; found C 34.31, H 1.88, N 5.55.

**3-Bromo-benzoic Acid (3,5-Dibromo-2,4-dihydroxy-benzylidene)-hydrazide (3k).** In the same manner as described in the preparation of **3c**, **3k** was prepared from 3-bromo-benzoic acid hydrazide and 3,5-dibromo-2,4-dihydroxy-benzaldehyde (**7**). Yield: 34.4%; mp 214–216 °C.  $^1H$  NMR (300 MHz, DMSO- $d_6$ ):  $\delta$  7.44 (t,  $J = 7.8$  Hz, 1H), 7.52 (s, 1H), 7.75 (d,  $J = 8.4$  Hz, 1H), 7.90 (d,  $J = 7.5$  Hz, 1H), 8.09 (s, 1H), 8.34 (s, 1H). EI-MS  $m/z$  490 ( $M^+$ ) 183 (100%). HRMS (EI)  $m/z$  calcd for  $M^+$  489.8163, found 489.8147. Anal. ( $C_{14}H_9Br_3N_2O_3$ ) calcd C 34.11, H 1.84, N 5.68; found C 34.31, H 1.79, N 5.64.

**Thiophene-2-carboxylic Acid (3,5-Dibromo-2,4-dihydroxy-benzylidene)-hydrazide (3l).** In the same manner as described in the preparation of **1**, **3l** was prepared from thiophene-2-carboxylic

acid hydrazide and 3,5-dibromo-2,4-dihydroxy-benzaldehyde (**7**). Yield: 54.8%; mp 244–246 °C.  $^1H$  NMR (300 MHz, DMSO- $d_6$ ):  $\delta$  7.25 (t,  $J = 4.5$  Hz, 1H), 7.76 (s, 1H), 7.91 (d,  $J = 4.8$  Hz, 2H), 8.43 (s, 1H). EI-MS  $m/z$  418 ( $M^+$ ) 111 (100%). HRMS (EI)  $m/z$  calcd for  $M^+$  417.8622, found 417.8607. Anal. ( $C_{14}H_9Br_3N_2O_3$ ) calcd C 34.31, H 1.92, N 6.67; found C 34.61, H 2.01, N 6.70.

**Naphthalene-2-carboxylic Acid (3,5-Dibromo-2,4-dihydroxy-benzylidene)-hydrazide (3m).** In the same manner as described in the preparation of **1**, **3m** was prepared from naphthalene-2-carboxylic acid hydrazide and 3,5-dibromo-2,4-dihydroxy-benzaldehyde (**7**). Yield: 44.9%; mp 243–244 °C.  $^1H$  NMR (300 MHz, DMSO- $d_6$ ):  $\delta$  7.66 (m, 2H), 7.78 (s, 1H), 8.04 (m, 4H), 8.52 (s, 1H), 8.57 (s, 1H). EI-MS  $m/z$  462 ( $M^+$ ) 155 (100%). HRMS (EI)  $m/z$  calcd for  $M^+$  461.9215, found 461.9207. Anal. ( $C_{18}H_{12}Br_2N_2O_3$ ) calcd C 46.58, H 2.61, N 6.04; found C 46.69, H 2.56, N 6.09.

**4-Methoxy-benzoic Acid (3,5-Dibromo-2,4-dihydroxy-benzylidene)-hydrazide (3n).** In the same manner as described in the preparation of **1**, **3n** was prepared from 4-methoxy-benzoic acid hydrazide and 3,5-dibromo-2,4-dihydroxy-benzaldehyde (**7**). Yield: 64.5%; mp 240–242 °C.  $^1H$  NMR (300 MHz, DMSO- $d_6$ ):  $\delta$  3.82 (s, 3H), 7.05 (d,  $J = 9.0$  Hz, 2H), 7.71 (s, 1H), 7.89 (d,  $J = 9.0$  Hz, 2H), 8.42 (s, 1H). EI-MS  $m/z$  442 ( $M^+$ ) 135 (100%). HRMS (EI)  $m/z$  calcd for  $M^+$  441.9164, found 441.9135. Anal. ( $C_{15}H_{12}Br_2N_2O_4$ ) calcd C 40.57, H 2.72, N 6.31; found C 40.88, H 2.69, N 5.82.

**Isonicotinic Acid (3,5-Dibromo-2,4-dihydroxy-benzylidene)-hydrazide (3o).** In the same manner as described in the preparation of **1**, **3o** was prepared from isonicotinic acid hydrazide and 3,5-dibromo-2,4-dihydroxy-benzaldehyde (**7**). Yield: 34.9%. HPLC: 100%,  $t_R = 2.86$  min, mp 242–244 °C.  $^1H$  NMR (300 MHz, DMSO- $d_6$ ):  $\delta$  7.81 (s, 1H), 7.85 (d,  $J = 6.0$  Hz, 2H), 8.49 (s, 1H), 8.81 (d,  $J = 6.0$  Hz, 2H). EI-MS  $m/z$  413 ( $M^+$ ) 106 (100%). HRMS (EI)  $m/z$  calcd for  $C_{13}H_9Br_2N_3O_3$  ( $M^+$ ) 412.9011, found 412.8996.

**Acetic Acid (3,5-Dibromo-2,4-dihydroxy-benzylidene)-hydrazide (3p).** In the same manner as described in the preparation of **1**, **3p** was prepared from acetic acid hydrazide and 3,5-dibromo-2,4-dihydroxy-benzaldehyde (**7**). Yield: 86.3%; mp 246–248 °C.  $^1H$  NMR (300 MHz, DMSO- $d_6$ ):  $\delta$  1.98 (s, 3H), 7.72 (s, 1H), 8.18 (s, 1H). EI-MS  $m/z$  350 ( $M^+$ ) 293 (100%). HRMS (EI)  $m/z$  calcd for  $M^+$  349.8902, found 349.8902. Anal. ( $C_9H_8Br_2N_2O_3$ ) calcd C 30.71, H 2.29, N 7.96; found C 30.76, H 2.28, N 7.52.

**4-tert-Butyl-benzoic Acid (3,5-Dibromo-2,4-dihydroxy-benzylidene)-hydrazide (3q).** In the same manner as described in the preparation of **1**, **3q** was prepared from 4-tert-butyl-benzoic acid hydrazide and 3,5-dibromo-2,4-dihydroxy-benzaldehyde (**7**). Yield: 50.7%; mp 240–242 °C.  $^1H$  NMR (300 MHz, DMSO- $d_6$ ):  $\delta$  1.32 (s, 9H), 7.56 (d,  $J = 8.4$  Hz, 2H), 7.75 (s, 1H), 7.87 (d,  $J = 8.4$  Hz, 2H), 8.46 (s, 1H). EI-MS  $m/z$  468 ( $M^+$ ) 161 (100%). HRMS (EI)  $m/z$  calcd for  $M^+$  467.9684, found 467.9682. Anal. ( $C_{18}H_{18}Br_2N_2O_3$ ) calcd C 45.98, H 3.86, N 5.96; found C 46.23, 4.14, N 5.65.

**(4-Hydroxy-phenyl)-acetic Acid (3,5-Dibromo-2,4-dihydroxy-benzylidene)-hydrazide (3r).** In the same manner as described in the preparation of **1**, **3r** was prepared from (4-hydroxy-phenyl)-acetic acid hydrazide and 3,5-dibromo-2,4-dihydroxy-benzaldehyde (**7**). Yield: 45.7%; HPLC: 99.45%,  $t_R = 3.53$  min, mp 241–242 °C.  $^1H$  NMR (300 MHz, DMSO- $d_6$ ):  $\delta$  3.43 (s, 2H), 6.69 (d,  $J = 8.4$  Hz, 2H), 7.09 (d,  $J = 8.4$  Hz, 2H), 7.72 (s, 1H), 8.23 (s, 1H). EI-MS  $m/z$  442 ( $M^+$ ) 107 (100%). HRMS (EI)  $m/z$  calcd for  $C_{15}H_{12}Br_2N_2O_4$  ( $M^+$ ) 441.9164, found 441.9171.

**4-Hydroxy-benzoic Acid (3,5-Dibromo-2,4-dihydroxy-benzylidene)-hydrazide (3a).** In the same manner as described in the preparation of **1**, **3a** was prepared from 4-hydroxy-benzoic acid hydrazide and 3,5-dibromo-2,4-dihydroxy-benzaldehyde (**7**). Yield: 76.1%; mp 275–276 °C.  $^1H$  NMR (300 MHz, DMSO- $d_6$ ):  $\delta$  6.88 (s, 1H), 6.91 (s, 1H), 7.74 (s, 1H), 7.84 (d,  $J = 9.0$  Hz, 2H), 8.44 (s, 1H). LRMS (EI)  $m/z$  428 ( $M^+$ ) 121 (100%). HRMS (EI)  $m/z$  calcd for  $M^+$  427.9007, found 427.9026. Anal. ( $C_{14}H_{10}Br_2N_2O_4$ ) calcd C 39.10, H 2.34, N 6.51; found C 39.27, H 2.48, N 6.38.

**4'-Hydroxy-biphenyl-4-carboxylic Acid (3,5-Dibromo-2,4-dihydroxy-benzylidene)-hydrazide (5b).** In the same manner as described in the preparation of **1**, **5b** was prepared from 4'-hydroxy-biphenyl-4-carboxylic acid hydrazide (**12g**) and 3,5-dibromo-2,4-dihydroxy-benzaldehyde (**7**). Yield: 68.1%; HPLC: 99.61%,  $t_R$  = 3.15 min, mp 113–114 °C.  $^1\text{H NMR}$  (300 MHz, DMSO- $d_6$ ):  $\delta$  6.91 (d,  $J$  = 7.8 Hz, 2H), 7.61 (d,  $J$  = 8.1 Hz, 2H), 7.77 (d,  $J$  = 5.4 Hz, 3H), 8.00 (d,  $J$  = 6.9 Hz, 2H), 8.50 (s, 1H). LRMS (EI)  $m/z$  504 ( $M^+$ ) 197 (100%). HRMS (EI)  $m/z$  calcd for  $C_{20}H_{14}Br_2N_2O_4$  ( $M^+$ ) 503.9320, found 503.9295.

**3,5-Bis(trifluoromethyl)-benzoic Acid (3,5-Dibromo-2,4-dihydroxy-benzylidene)-hydrazide (5c).** In the same manner as described in the preparation of **1**, **5c** was prepared from 3,5-bis(trifluoromethyl)-benzoic acid hydrazide and 3,5-dibromo-2,4-dihydroxy-benzaldehyde (**7**). Yield: 61.5%; mp 240–242 °C.  $^1\text{H NMR}$  (300 MHz, DMSO- $d_6$ ):  $\delta$  7.78 (d,  $J$  = 12.0 Hz, 1H), 8.34 (s, 1H), 8.48 (s, 1H), 8.57 (s, 2H). LRMS (EI)  $m/z$  548 ( $M^+$ ) 241 (100%). HRMS (EI)  $m/z$  calcd for  $M^+$  547.8806, found 547.8818. Anal. ( $C_{16}H_8Br_2F_6N_2O_3$ ) calcd C 34.94, H 1.47, N 5.09; found 35.30, H 1.47, N 5.09.

**4-Phenoxy-benzoic Acid (3,5-Dibromo-2,4-dihydroxy-benzylidene)-hydrazide (5d).** In the same manner as described in the preparation of **1**, **5d** was prepared from 4-phenoxy-benzoic acid hydrazide (**12d**) and 3,5-dibromo-2,4-dihydroxy-benzaldehyde (**7**). Yield: 79.2%; mp 113–114 °C.  $^1\text{H NMR}$  (300 MHz, DMSO- $d_6$ ):  $\delta$  7.09–7.15 (m, 3H), 7.24 (t, 1H), 7.43–7.50 (m, 3H), 7.76 (s, 1H), 7.99 (d,  $J$  = 9 Hz, 2H), 8.46 (s, 1H). LRMS (EI)  $m/z$  504 ( $M^+$ ) 197 (100%). HRMS (EI)  $m/z$  calcd for  $M^+$  503.9320, found 503.9302. Anal. ( $C_{20}H_{14}Br_2N_2O_4$ ) calcd C 47.46, H 2.79, N 5.53; found C 47.56, H 2.71, N 5.74.

**Biphenyl-4-carboxylic Acid (3,5-Dibromo-2,4-dihydroxy-benzylidene)-hydrazide (5e).** In the same manner as described in the preparation of **1**, **5e** was prepared from biphenyl-4-carboxylic acid hydrazide (**12b**) and 3,5-dibromo-2,4-dihydroxy-benzaldehyde (**7**). Yield: 77.2%; mp 178–179 °C.  $^1\text{H NMR}$  (300 MHz, DMSO- $d_6$ ):  $\delta$  7.44 (t, 1H), 7.52 (t, 2H), 7.77 (t, 3H), 7.87 (d,  $J$  = 8.7 Hz, 2H), 8.06 (d,  $J$  = 8.4 Hz, 2H), 8.51 (s, 1H). LRMS (EI)  $m/z$  488 ( $M^+$ ) 181 (100%). HRMS (EI)  $m/z$  calcd for  $M^+$ , 487.9371, found 487.9348. Anal. ( $C_{20}H_{14}Br_2N_2O_3$ ) calcd C 49.01, H 2.88, N 5.72; found C 48.96, H 2.79, N 5.67.

**9H-Fluorene-2-carboxylic Acid (3,5-Dibromo-2,4-dihydroxy-benzylidene)-hydrazide (5f).** In the same manner as described in the preparation of **1**, **5f** was prepared from 9H-fluorene-2-carboxylic acid hydrazide (**12f**) and 3,5-dibromo-2,4-dihydroxy-benzaldehyde (**7**). Yield: 65.6%.  $^1\text{H NMR}$  (300 MHz, DMSO- $d_6$ ):  $\delta$  3.40 (s, 2H), 7.42(s, 2H), 7.64 (s, 1H), 7.76 (s, 1H), 8.03 (d,  $J$  = 6.6 Hz, 2H), 8.18 (s, 1H), 8.49 (s, 1H). EI-MS  $m/z$  500 ( $M^+$ ) 193 (100%). HRMS (EI)  $m/z$  calcd for  $M^+$  499.9371, found 499.9381. Anal. ( $C_{21}H_{14}Br_2N_2O_3$ ) calcd C 50.23, H 2.81, N 5.58; found C 50.38, H 2.87, N 5.47.

**1-Hydroxy-naphthalene-2-carboxylic Acid (3,5-Dibromo-2,4-dihydroxy-benzylidene)-hydrazide (5g).** In the same manner as described in the preparation of **1**, **5g** was prepared from 1-hydroxy-2-naphthoic acid hydrazide (**12a**) and 3,5-dibromo-2,4-dihydroxy-benzaldehyde (**7**). Yield: 68.3%; HPLC: 96.58%,  $t_R$  = 13.43 min, mp 132–133 °C.  $^1\text{H NMR}$  (300 MHz, DMSO- $d_6$ ):  $\delta$  7.47 (d,  $J$  = 8.7 Hz, 1H), 7.59 (t, 1H), 7.68 (t, 1H), 7.80 (s, 1H), 7.89–7.97 (m, 2H), 8.31 (d,  $J$  = 8.1 Hz, 1H), 8.57 (s, 1H). LRMS (EI)  $m/z$  478 ( $M^+$ ) 171 (100%). HRMS (EI)  $m/z$  calcd  $C_{18}H_{12}Br_2N_2O_4$  ( $M^+$ ) 477.9164, found 477.9139.

**3-Hydroxy-naphthalene-2-carboxylic Acid (3,5-Dibromo-2,4-dihydroxy-benzylidene)-hydrazide (5h).** In the same manner as described in the preparation of **1**, **5h** was prepared from 3-hydroxy-2-naphthoic acid hydrazide and 3,5-dibromo-2,4-dihydroxy-benzaldehyde (**7**). Yield: 62.7%; mp 241–242 °C.  $^1\text{H NMR}$  (300 MHz, DMSO- $d_6$ ):  $\delta$  7.28–7.75 (m, 2H), 7.76–7.71 (m, 1H), 7.82 (dd,  $J$  = 9.6 Hz and  $J$  = 9 Hz, 2H), 7.98 (dd,  $J$  = 10.8 Hz and  $J$  = 7.8 Hz, 1H), 8.43 (d,  $J$  = 15.3 Hz, 1H), 8.57 (m, 1H). LRMS (EI)  $m/z$  478 ( $M^+$ ) 171 (100%); HRMS (EI)  $m/z$  calcd for  $M^+$  477.9164, found 477.9153. Anal. ( $C_{18}H_{12}Br_2N_2O_4$ ) calcd C 45.03, H 2.52, N 5.83; found C 44.67, H 2.45, N 5.76.

**6-Hydroxy-naphthalene-2-carboxylic Acid (3,5-Dibromo-2,4-dihydroxy-benzylidene)-hydrazide (5i).** In the same manner as described in the preparation of **1**, **5i** was prepared from 6-hydroxy-2-naphthoic acid hydrazide (**12e**) and 3,5-dibromo-2,4-dihydroxy-benzaldehyde (**7**). Yield: 52%; HPLC: 95.73%,  $t_R$  = 2.56 min, mp 113–114 °C.  $^1\text{H NMR}$  (300 MHz, DMSO- $d_6$ ):  $\delta$  7.20 (t, 2H), 7.76 (d,  $J$  = 5.4 Hz, 1H), 7.83 (d,  $J$  = 8.7 Hz, 1H), 7.93 (t, 2H), 8.46 (s, 1H), 8.51 (s, 1H). LRMS (EI)  $m/z$  478 ( $M^+$ ) 171 (100%). HRMS (EI)  $m/z$  calcd  $C_{18}H_{12}Br_2N_2O_4$  ( $M^+$ ) 477.9164, found 477.9139.

**6-Bromo-naphthalene-2-carboxylic Acid (3,5-Dibromo-2,4-dihydroxy-benzylidene)-hydrazide (5j).** In the same manner as described in the preparation of **1**, **5j** was prepared from 6-bromo-2-naphthoic acid hydrazide (**12c**) and 3,5-dibromo-2,4-dihydroxy-benzaldehyde (**7**). Yield: 59.4%; mp 166–167 °C.  $^1\text{H NMR}$  (300 MHz, DMSO- $d_6$ ):  $\delta$  7.75 (t, 2H), 8.07 (d,  $J$  = 7.8 Hz, 3H), 8.32 (s, 1H), 8.51 (s, 1H), 8.59 (s, 1H). LRMS (EI)  $m/z$  540 ( $M^+$ ) 235 (100%). HRMS (EI)  $m/z$  calcd for  $M^+$  539.8320, found 539.8250. Anal. ( $C_{18}H_{11}Br_3N_2O_3$ ) calcd C 39.81, H 2.04, N 5.16; found C 40.06, H 2.28, N 5.01.

**N-(3,5-Bis(trifluoromethyl)phenyl)-3-(2,3,4-trimethoxyphenyl)Acrylamide (5l).** 3-(2,3,4-Trimethoxyphenyl)acrylic acid (238 mg, 1.0 mmol) and 3,5-bis(trifluoromethyl)aniline (229 mg, 1.0 mmol) was dissolved in  $\text{CH}_2\text{Cl}_2$  and pyridine. After 5 h, plenty of water was added and the organic layer was extracted with EtOAc for three times, and the combined organic layers were washed and then dried over  $\text{MgSO}_4$ . After flash chromatography with ethyl acetate–petroleum (1:5, v/v) and purified using RP-HPLC to afford the final compound **5l** was obtained as a white solid, yield 67.6%; HPLC: 99.00%,  $t_R$  = 4.00 min.  $^1\text{H NMR}$  (300 MHz, DMSO- $d_6$ ):  $\delta$  3.78 (s, 3H), 3.85 (s, 6H), 6.75 (d,  $J$  = 15.6 Hz, 1H), 6.93 (d,  $J$  = 8.4 Hz, 1H), 7.38 (d,  $J$  = 8.7 Hz, 1H), 7.75 (d,  $J$  = 15.9 Hz, 1H), 8.36 (s, 2H). EI-MS  $m/z$  449 ( $M^+$ ) 221 (100%). HRMS (EI)  $m/z$  calcd for  $M^+$  449.1062, found 449.1035.

**1-(2-Methoxy-ethyl)-3-phenyl-thiourea (15a). Representative Procedure for 15a–q and 5k.** Isothiocyanato-benzene (1.35 g, 0.01 mol) was dissolved in toluene, and then 2-methoxyethylamine (751 mg, 0.01 mol) was added, and after a while, plenty of white precipitation appeared. Stirring was continued for 1 h. The precipitation was collected by filtration, washed with toluene, and dried to afford **15a** (1.997 g, 95.0%) as white powder.  $^1\text{H NMR}$  ( $\text{CDCl}_3$ ):  $\delta$  3.30 (s, 3H), 3.53 (t,  $J$  = 8.4 Hz, 2H), 3.82 (s, br, 2H), 7.19–7.29 (m, 3H), 7.38–7.43 (m, 2H).

**1-(2-Methoxy-ethyl)-3-(4-methoxy-phenyl)-thiourea (15b).**  $^1\text{H NMR}$  ( $\text{CDCl}_3$ ):  $\delta$  3.29 (s, 3H), 3.52 (t,  $J$  = 9.9 Hz, 2H), 3.80–3.82 (m, 5H), 6.93 (d,  $J$  = 9.0 Hz, 2H), 7.14 (d,  $J$  = 8.7 Hz, 2H).

**1-(4-Bromo-phenyl)-3-(2-methoxy-ethyl)-thiourea (15c).**  $^1\text{H NMR}$  ( $\text{CDCl}_3$ ):  $\delta$  3.34 (s, 3H), 3.55 (t, 2H), 3.81 (t, 2H), 7.11 (d,  $J$  = 9.3 Hz, 2H), 7.53 (d,  $J$  = 8.4 Hz, 2H).

**1-(2-Methoxy-ethyl)-3-naphthalen-1-yl-thiourea (15d).**  $^1\text{H NMR}$  ( $\text{CDCl}_3$ ):  $\delta$  3.13 (s, 3H), 3.44 (t,  $J$  = 9.6 Hz, 2H), 3.79 (t,  $J$  = 3.9 Hz, 2H), 7.43–7.59 (m, 4H), 7.87–7.99 (m, 3H).

**1-(2-Methoxy-ethyl)-3-(4-trifluoromethyl-phenyl)-thiourea (15e).**  $^1\text{H NMR}$  ( $\text{CDCl}_3$ ):  $\delta$  3.37 (s, 3H), 3.59 (t,  $J$  = 9.3 Hz, 2H), 3.81 (t,  $J$  = 7.2 Hz, 2H), 7.40 (d,  $J$  = 8.1 Hz, 2H), 7.65 (d,  $J$  = 8.1 Hz, 2H).

**1-(3-Dimethylamino-propyl)-3-phenyl-thiourea (15f).**  $^1\text{H NMR}$  ( $\text{CDCl}_3$ ):  $\delta$  1.29 (t, 2H), 1.40 (s, 6H), 1.96 (t, 2H), 3.38 (t, 2H), 6.85–6.94 (m, 2H), 7.02–7.07 (m, 2H), 7.36 (s, 1H).

**1-(2-Diethylamino-ethyl)-3-phenyl-thiourea (15g).**  $^1\text{H NMR}$  ( $\text{CDCl}_3$ ):  $\delta$  0.78 (t, 6H), 2.39 (q, 4H), 2.52 (t,  $J$  = 15.6 Hz, 2H), 3.60 (t, 2H), 7.12–7.21 (m, 2H), 7.36–7.41 (m, 2H), 7.76 (s, 1H).

**1-Phenyl-3-(2-pyrrolidin-1-yl-ethyl)-thiourea (15h).**  $^1\text{H NMR}$  ( $\text{CDCl}_3$ ):  $\delta$  1.53 (m, 4H), 2.40 (m, 4H), 2.58 (t,  $J$  = 5.7 Hz, 2H), 3.51 (t,  $J$  = 5.7 Hz, 2H), 7.07–7.16 (m, 2H), 7.19–7.24 (m, 2H), 7.77 (s, 1H).

**1-(2-Methoxy-ethyl)-3-(2-methoxy-phenyl)-thiourea (15i).**  $^1\text{H NMR}$  ( $\text{CDCl}_3$ ):  $\delta$  3.33 (s, 3H), 3.56 (t,  $J$  = 10.2 Hz, 2H), 3.85 (s, 5H), 6.98–6.95 (m, 2H), 7.22 (m, 1H), 7.26 (m, 2H).

**1-(2-Methoxy-ethyl)-3-(3-methoxy-phenyl)-thiourea (15j).**  $^1\text{H NMR}$  ( $\text{CDCl}_3$ ):  $\delta$  3.32 (s, 3H), 3.54 (t,  $J$  = 9.6 Hz, 2H), 3.80 (s, 3H), 3.83 (t, 2H), 6.76–6.83 (m, 3H), 7.28–7.33 (m, 1H).

**1-(2-Methoxy-ethyl)-3-(2-trifluoromethyl-phenyl)-thiourea (15k).**  $^1\text{H NMR}$  ( $\text{CDCl}_3$ ):  $\delta$  3.31 (s, 3H), 3.54 (t,  $J = 9.9$  Hz, 2H), 3.79 (t, 2H), 7.40–7.51 (m, 2H), 7.54–7.84 (m, 2H).

**1-(2-Methoxy-ethyl)-3-(3-trifluoromethyl-phenyl)-thiourea (15l).**  $^1\text{H NMR}$  ( $\text{CDCl}_3$ ):  $\delta$  3.34 (s, 3H), 3.57 (t,  $J = 4.2$  Hz, 2H), 3.80 (t, 2H), 7.486 (m, 3H), 7.54 (s, 1H).

**1-(2-Bromo-phenyl)-3-(2-methoxy-ethyl)-thiourea (15m).**  $^1\text{H NMR}$  ( $\text{CDCl}_3$ ):  $\delta$  3.32 (s, 3H), 3.56 (t,  $J = 9.9$  Hz, 2H), 3.82 (t, 2H), 7.16 (m, 1H), 7.36–7.43 (m, 2H), 7.67 (d, 1H).

**1-(3-Bromo-phenyl)-3-(2-methoxy-ethyl)-thiourea (15n).**  $^1\text{H NMR}$  ( $\text{CDCl}_3$ ):  $\delta$  3.36 (s, 3H), 3.56 (t,  $J = 9.9$  Hz, 2H), 3.81 (t, 2H), 7.19 (m, 1H), 7.25–7.30 (m, 1H), 7.38–7.40 (m, 2H).

**1-(2-Fluoro-phenyl)-3-(2-methoxy-ethyl)-thiourea (15o).**  $^1\text{H NMR}$  ( $\text{CDCl}_3$ ):  $\delta$  3.33 (s, 3H), 3.56 (t,  $J = 9.6$  Hz, 2H), 3.80 (t, 2H), 6.52–6.61 (m, 1H), 7.13–7.36 (m, 2H), 7.56–7.57 (m, 1H).

**1-(4-Fluoro-phenyl)-3-(2-methoxy-ethyl)-thiourea (15p).**  $^1\text{H NMR}$  ( $\text{CDCl}_3$ ):  $\delta$  3.32 (s, 3H), 3.54 (t,  $J = 9.9$  Hz, 2H), 3.81 (t, 2H), 7.08–7.13 (m, 2H), 7.21–7.27 (m, 2H).

**1-(3-Fluoro-phenyl)-3-(2-methoxy-ethyl)-thiourea (15q).**  $^1\text{H NMR}$  ( $\text{CDCl}_3$ ):  $\delta$  3.36 (s, 3H), 3.58 (t,  $J = 9.9$  Hz, 2H), 3.84 (t, 2H), 6.97–7.05 (m, 3H), 7.37–7.39 (m, 1H).

**1-(3,4,5-Trimethoxybenzyl)-3-(3,5-bis(trifluoromethyl)phenyl) Thiourea (5k).** In the same manner as described in the preparation of **15a**, **5k** was prepared from 1-isothiocyanato-3,5-bis(trifluoromethyl) benzene and (3,4,5-trimethoxyphenyl) methanamine. Yield: 90.5%; HPLC: 100.00%,  $t_R = 2.39$  min.  $^1\text{H NMR}$  (300 MHz,  $\text{DMSO}-d_6$ ):  $\delta$  3.65 (s, 3H), 3.78 (s, 6H), 4.68 (s, 2H), 6.72 (s, 2H), 7.76 (s, 1H), 8.27 (d,  $J = 3.3$  Hz, 1H). EI-MS  $m/z$  468 ( $\text{M}^+$ ) 181 (100%). HRMS (EI)  $m/z$  calcd for  $\text{C}_{15}\text{H}_{12}\text{Br}_2\text{N}_2\text{O}_4$  ( $\text{M}^+$ ) 468.0942, found 468.0936.

**3-(2-Methoxy-ethyl)-2-phenylimino-thiazolidin-4-one (16a).** **Representative Procedure for 16a–q.** 1-(2-Methoxy-ethyl)-3-phenyl-thiourea (**15a**) (2.120 g, 16.08 mmol) was dissolved in EtOH, and then anhydrous sodium acetate (1.643 g, 32.17 mmol) and chloroacetic acid (1.190 g, 20.10 mmol) were added in sequence. The suspension was refluxed for 12 h, and then the solvent was evaporated. Water was added and the aqueous layer was back-extracted with ethyl acetate. The organic layer was washed with saturated sodium bicarbonate and brine. The combined organic extracts were dried over  $\text{Na}_2\text{SO}_4$ , filtered through cotton, and concentrated in vacuo, and then purified by chromatography with EtOAc/petroleum ether (1:15, v/v) to give 2.235 g (89.3%) of **16a** as yellow–white oil.  $^1\text{H NMR}$  ( $\text{CDCl}_3$ ):  $\delta$  3.39 (s, 3H), 3.71 (t,  $J = 11.4$  Hz, 2H), 3.83 (s, 2H), 4.09 (t,  $J = 11.4$  Hz, 2H), 6.95–6.97 (m, 2H), 7.14 (t, 1H), 7.32–7.37 (m, 2H).

**3-(2-Methoxy-ethyl)-2-(4-methoxy-phenylimino)-thiazolidin-4-one (16b).**  $^1\text{H NMR}$  ( $\text{CDCl}_3$ ):  $\delta$  3.39 (s, 3H), 3.70 (t,  $J = 11.1$  Hz, 2H), 3.81 (s, 2H), 4.07 (t,  $J = 11.1$  Hz, 2H), 6.89–6.90 (m, 4H).

**2-(4-Bromo-phenylimino)-3-(2-methoxy-ethyl)-thiazolidin-4-one (16c).**  $^1\text{H NMR}$  ( $\text{CDCl}_3$ ):  $\delta$  3.38 (s, 3H), 3.69 (t,  $J = 11.1$  Hz, 2H), 3.84 (s, 2H), 4.06 (t,  $J = 10.8$  Hz, 2H), 6.84 (d,  $J = 8.7$  Hz, 2H), 7.45 (d,  $J = 8.7$  Hz, 2H).

**3-(2-Methoxy-ethyl)-2-(naphthalen-1-ylimino)-thiazolidin-4-one (16d).**  $^1\text{H NMR}$  ( $\text{CDCl}_3$ ):  $\delta$  3.46 (s, 3H), 3.83 (m, 4H), 4.24 (t,  $J = 5.7$  Hz, 2H), 7.04 (d,  $J = 7.5$ , 1H), 7.40–7.51 (m, 3H), 7.66 (d,  $J = 8.4$  Hz, 1H), 7.84–7.88 (m, 1H), 7.94 (d,  $J = 7.8$  Hz, 1H).

**3-(2-Methoxy-ethyl)-2-(4-trifluoromethyl-phenylimino)-thiazolidin-4-one (16e).**  $^1\text{H NMR}$  ( $\text{CDCl}_3$ ):  $\delta$  3.38 (s, 3H), 3.70 (t,  $J = 11.1$  Hz, 2H), 3.84 (s, 2H), 4.07 (t,  $J = 11.1$  Hz, 2H), 7.03 (d,  $J = 8.1$  Hz, 2H), 7.59 (d,  $J = 8.1$  Hz, 2H).

**3-(3-Dimethylamino-propyl)-2-phenylimino-thiazolidin-4-one (16f).**  $^1\text{H NMR}$  ( $\text{CDCl}_3$ ):  $\delta$  1.80 (t,  $J = 15.3$  Hz, 2H), 2.23 (s, 6H), 2.49 (t,  $J = 15.9$  Hz, 2H), 3.54 (s, 2H), 3.63 (t,  $J = 14.1$  Hz, 2H), 6.67 (d,  $J = 8.1$  Hz, 2H), 6.87 (t,  $J = 7.5$  Hz, 1H), 6.99–7.09 (m, 1H).

**3-(2-Diethylamino-ethyl)-2-phenylimino-thiazolidin-4-one (16g).**  $^1\text{H NMR}$  ( $\text{CDCl}_3$ ):  $\delta$  0.76 (t,  $J = 14.1$  Hz, 6H), 2.38 (q, 4H), 2.56 (t,  $J = 13.5$  Hz, 2H), 3.47 (s, 2H), 3.64 (t,  $J = 14.1$  Hz, 2H), 6.61 (d,  $J = 8.1$  Hz, 2H), 6.78 (t,  $J = 4.7$  Hz, 1H), 6.99 (t, 2H).

**2-Phenylimino-3-(2-pyrrolidin-1-yl-ethyl)-thiazolidin-4-one (16h).**  $^1\text{H NMR}$  ( $\text{CDCl}_3$ ):  $\delta$  1.92 (m, 4H), 3.01 (m, 4H), 3.14 (t, 2H), 3.87 (s, 2H), 4.09 (t,  $J = 12.6$  Hz, 2H), 6.98 (dd,  $J = 1.2$  Hz, and  $J = 1.5$  Hz, 2H), 7.11 (m, 1H), 7.30–7.34 (m, 2H).

**3-(2-Methoxy-ethyl)-2-(2-methoxy-phenylimino)-thiazolidin-4-one (16i).**  $^1\text{H NMR}$  ( $\text{CDCl}_3$ ):  $\delta$  3.40 (s, 3H), 3.75 (t,  $J = 11.1$  Hz, 2H), 3.82 (m, 5H), 4.12 (t,  $J = 11.1$  Hz, 2H), 6.89–6.95 (m, 3H), 7.13 (m, 1H).

**3-(2-Methoxy-ethyl)-2-(3-methoxy-phenylimino)-thiazolidin-4-one (16j).**  $^1\text{H NMR}$  ( $\text{CDCl}_3$ ):  $\delta$  3.39 (s, 3H), 3.71 (t,  $J = 11.1$  Hz, 2H), 3.82 (s, 2H), 4.07 (t,  $J = 11.4$  Hz, 2H), 6.51–6.57 (m, 2H), 6.68–6.71 (m, 1H), 7.20–7.22 (m, 1H).

**3-(2-Methoxy-ethyl)-2-(2-trifluoromethyl-phenylimino)-thiazolidin-4-one (16k).**  $^1\text{H NMR}$  ( $\text{CDCl}_3$ ):  $\delta$  3.38 (s, 3H), 3.72 (t,  $J = 11.4$  Hz, 2H), 3.87 (s, 2H), 4.07 (t,  $J = 11.7$  Hz, 2H), 7.02 (d,  $J = 8.1$  Hz, 1H), 7.22–7.26 (m, 1H), 7.50 (m, 1H), 7.67 (d,  $J = 7.8$  Hz, 1H).

**3-(2-Methoxy-ethyl)-2-(3-trifluoromethyl-phenylimino)-thiazolidin-4-one (16l).**  $^1\text{H NMR}$  ( $\text{CDCl}_3$ ):  $\delta$  3.39 (s, 3H), 3.71 (t,  $J = 11.4$  Hz, 2H), 3.86 (s, 2H), 4.10 (t, 2H), 7.16 (d, 1H), 7.24 (d, 1H), 7.41–7.46 (m, 2H).

**2-(2-Bromo-phenylimino)-3-(2-methoxy-ethyl)-thiazolidin-4-one (16m).**  $^1\text{H NMR}$  ( $\text{CDCl}_3$ ):  $\delta$  3.40 (s, 3H), 3.79 (t,  $J = 11.4$  Hz, 2H), 3.86 (s, 2H), 4.11 (t,  $J = 11.4$  Hz, 2H), 6.95–6.97 (m, 2H), 7.27 (t,  $J = 7.8$  Hz, 1H), 7.61 (d,  $J = 8.1$  Hz, 1H).

**2-(3-Bromo-phenylimino)-3-(2-methoxy-ethyl)-thiazolidin-4-one (16n).**  $^1\text{H NMR}$  ( $\text{CDCl}_3$ ):  $\delta$  3.38 (s, 3H), 3.69 (t,  $J = 11.1$  Hz, 2H), 3.85 (s, 2H), 4.06 (t,  $J = 11.1$  Hz, 2H), 6.90 (d, 1H), 7.13 (s, 1H), 7.21–7.23 (m, 1H), 7.26 (m, 1H).

**2-(2-Fluoro-phenylimino)-3-(2-methoxy-ethyl)-thiazolidin-4-one (16o).**  $^1\text{H NMR}$  ( $\text{CDCl}_3$ ):  $\delta$  3.39 (s, 3H), 3.73 (t,  $J = 11.4$  Hz, 2H), 3.86 (s, 2H), 4.10 (t,  $J = 11.1$  Hz, 2H), 6.97–7.00 (m, 1H), 7.10–7.12 (m, 3H).

**2-(4-Fluoro-phenylimino)-3-(2-methoxy-ethyl)-thiazolidin-4-one (16p).**  $^1\text{H NMR}$  ( $\text{CDCl}_3$ ):  $\delta$  3.39 (s, 3H), 3.70 (t,  $J = 11.4$  Hz, 2H), 3.83 (s, 2H), 4.06 (t,  $J = 11.4$  Hz, 2H), 6.89–6.95 (m, 2H), 7.00–7.06 (m, 2 H).

**2-(3-Fluoro-phenylimino)-3-(2-methoxy-ethyl)-thiazolidin-4-one (16q).**  $^1\text{H NMR}$  ( $\text{CDCl}_3$ ):  $\delta$  3.38 (s, 3H), 3.69 (t,  $J = 8.4$  Hz, 2H), 3.84 (s, 2H), 4.06 (t,  $J = 8.4$  Hz, 2H), 6.66–6.70 (m, 1H), 6.73–6.75 (m, 1H), 6.81–6.86 (t, 1H), 7.26–7.32 (m, 1H).

**5-Amino-2-chloro-benzoic Acid Methyl Ester (18a).** A 100 mL round-bottom flask with a magnetic stir bar was charged with 5-amino-2-chloro-benzoic acid (3.433 g, 0.02 mol),  $\text{H}_2\text{SO}_4$  (catalysis), and 50 mL of MeOH, and the solution was refluxed for 5 h. MeOH was evaporated in vacuo. Water was added, and the aqueous layer was back-extracted with ethyl acetate. The organic layer was washed with saturated sodium bicarbonate and brine. The combined organic extracts were dried over  $\text{Na}_2\text{SO}_4$ , filtered through cotton, and concentrated in vacuo, yielding **18a** (3.19 g, 93.0%) as yellow oil.  $^1\text{H NMR}$  ( $\text{CDCl}_3$ ):  $\delta$  3.97 (s, 3H), 6.98 (d, 1H), 7.55 (d, 1H), 7.86 (d, 1H).

**3-Amino-4-chloro-benzoic acid methyl ester (18b).** In the same manner as described in the preparation of **18a**, **18b** was prepared from 3-amino-4-chloro-benzoic acid. Yield: 87.7%.  $^1\text{H NMR}$  ( $\text{CDCl}_3$ ):  $\delta$  3.90 (s, 3H), 7.15 (d, 2H), 7.53 (d, 1H).

**2-Chloro-5-(5-formyl-furan-2-yl)-benzoic Acid Methyl Ester (19a).** A mixture of 5-amino-2-chloro-benzoic acid methyl ester (**18a**) (8.67 mmol), hydrochloric acid (15%, 5.2 mL), and water (9 mL) was heated to get a clear solution. The solution was cooled to 0 °C and was diazotized by the addition of sodium nitrite solution (30%, 2.0 mL). The cold clear solution of the diazonium salt was collected by filtration and was treated with 2-furfuraldehyde (0.72 mL, 8.67 mmol) and water (5 mL). To this, an aqueous solution of cupric chloride (219 mg in 1 mL of water) was added dropwise with stirring. Stirring was continued for 4 h at room temperature

and the precipitated solid was collected by filtration. The crude compound **19a** was recrystallized from a mixture of ethanol and dioxane. Yield: 67.7%. <sup>1</sup>H NMR (CDCl<sub>3</sub>): δ 3.98 (s, 3H), 6.91 (d, *J* = 3.6 Hz, 1H), 7.345 (d, *J* = 3.9 Hz, 1H), 7.54 (d, *J* = 8.4 Hz, 1H), 7.85 (d, *J* = 2.1 Hz, 1H), 8.26 (d, *J* = 2.4 Hz, 1H), 9.68 (s, 1H).

**4-Chloro-3-(5-formyl-furan-2-yl)-benzoic Acid Methyl Ester (19b).** In the same manner as described in the preparation of **19a**, **19b** was prepared from 3-amino-4-chloro-benzoic acid methyl ester (**18b**) and 2-furfuraldehyde, and then the precipitated solid was collected by filtration and then purified by chromatography with EtOAc-petroleum ether (1:15, v/v). Yield: 65.3%. <sup>1</sup>H NMR (CDCl<sub>3</sub>): δ 3.97 (s, 3H), 7.34–7.38 (m, 2H), 7.58 (d, *J* = 8.1 Hz, 1H), 7.99 (dd, *J* = 2.1 Hz and 1.8 Hz, 1H), 8.64 (d, *J* = 2.4 Hz, 1H), 9.76 (s, 1H).

**5-(4-Chloro-phenyl)-furan-2-carbaldehyde (19c).**<sup>47</sup> In the same manner as described in the preparation of **19a**, **19c** was prepared from 4-chloro aniline and 2-furfuraldehyde, and then the precipitated solid was collected by filtration and then purified by chromatography with EtOAc/petroleum ether (1:15, v/v). Yield: 60.1%. <sup>1</sup>H NMR (CDCl<sub>3</sub>): δ 6.83 (d, *J* = 3.9 Hz, 1H), 7.32 (d, *J* = 3.9 Hz, 1H), 7.42 (d, *J* = 8.7 Hz, 2H), 7.76 (d, *J* = 8.7 Hz, 2H), 9.67 (s, 1H).

**2-Chloro-5-{5-[3-(2-methoxy-ethyl)-4-oxo-2-phenylimino-thiazolidin-5-ylidenemethyl]-furan-2-yl}-benzoic Acid Methyl Ester (4c).** A mixture of 3-(2-methoxy-ethyl)-2-phenylimino-thiazolidin-4-one (**16a**) (1.254 g, 5 mmol), 2-chloro-5-(5-formyl-furan-2-yl)-benzoic acid methyl ester (**19a**) (1.327 g, 5 mmol), hexahydropyridine (0.58 mL, 5.75 mmol), and 35 mL of EtOH were refluxed for 11–12 h. The reaction mixture was cooled to room temperature and the precipitated solid was collected by filtration, washed with EtOH, and purified using RP-HPLC to afford the final compound **4c** as yellow powder. Yield: 60.1%; mp 150–151 °C. <sup>1</sup>H NMR (DMSO-*d*<sub>6</sub>): δ 3.30 (s, 3H), 3.68 (t, *J* = 11.7 Hz, 2H), 3.81 (s, 3H), 4.06 (t, *J* = 5.4 Hz, 2H), 7.05–7.07 (m, 2H), 7.12 (d, *J* = 3.3 Hz, 1H), 7.24 (m, 1H), 7.32 (d, *J* = 1.8 Hz, 1H), 7.45 (t, 2H), 7.56 (d, *J* = 7.2 Hz, 2H), 7.72 (m, 1H), 7.94 (d, *J* = 2.4 Hz, 1H). EI-MS *m/z* 496 (M<sup>+</sup>) 292 (100%). HRMS (EI) *m/z* calcd for M<sup>+</sup> 496.0860, found 496.0860. Anal. (C<sub>25</sub>H<sub>21</sub>ClN<sub>2</sub>O<sub>5</sub>S) calcd C 60.42, H 4.26, N 5.64; found C 60.26, H 4.05, N 5.57.

**2-Chloro-5-{5-[3-(2-methoxy-ethyl)-4-oxo-2-phenylimino-thiazolidin-5-ylidenemethyl]-furan-2-yl}-benzoic acid (2).** 2-Chloro-5-{5-[3-(2-methoxy-ethyl)-4-oxo-2-phenylimino-thiazolidin-5-ylidenemethyl]-furan-2-yl}-benzoic acid methyl ester (**4c**) (200 mg, 0.40 mmol) in a solvent of THF (15 mL) was added aqueous LiOH (84.4 mg, 2.01 mmol) solution, and the mixture was stirred at room temperature for 6 h. After the removal of THF, water was added to the mixture and then 10% HCl was added until PH = 6 and yellow solid was precipitated. The precipitation was collected by filtration and washed with MeOH and purified using RP-HPLC to afford the final compound **2** (182 mg, 91.2%) as yellow powder: mp 210–212 °C. HPLC: 97.28%, *t*<sub>R</sub> = 4.22 min. <sup>1</sup>H NMR (DMSO-*d*<sub>6</sub>): δ 3.30 (s, 3H), 3.68 (t, *J* = 11.7 Hz, 2H), 4.06 (t, *J* = 5.7 Hz, 2H), 7.07 (d, *J* = 7.5 Hz, 2H), 7.13 (d, *J* = 3.6 Hz, 1H), 7.25 (m, 1H), 7.34 (d, *J* = 3.0 Hz, 1H), 7.46 (t, 2H), 7.56 (t, 2H), 7.69 (m, 1H), 7.96 (d, *J* = 2.1 Hz, 1H). EI-MS *m/z* 482 (M<sup>+</sup>) 278 (100%). HRMS (EI) *m/z* calcd for C<sub>24</sub>H<sub>19</sub>ClN<sub>2</sub>O<sub>5</sub>S (M<sup>+</sup>) 482.0687, found 482.0703.

**2-Chloro-5-{5-[3-(2-methoxy-ethyl)-2-(4-methoxy-phenylimino)-4-oxo-thiazolidin-5-ylidenemethyl]-furan-2-yl}-benzoic Acid Methyl Ester (4d).** In the same manner as described in the preparation of **4c**, **4d** was prepared from 3-(2-methoxy-ethyl)-2-(4-methoxy-phenylimino)-thiazolidin-4-one (**16b**), 2-chloro-5-(5-formyl-furan-2-yl)-benzoic acid methyl ester (**19a**), and hexahydropyridine (0.58 mL, 5.75 mmol). Yield: 64.6%; mp 86–88 °C. HPLC: 95.99%, *t*<sub>R</sub> = 8.76 min. <sup>1</sup>H NMR (DMSO-*d*<sub>6</sub>): δ 3.29 (s, 3H), 3.67 (t, *J* = 11.1 Hz, 2H), 3.79 (s, 6H), 4.05 (t, *J* = 11.4 Hz, 2H), 7.01 (s, 4H), 7.12 (d, *J* = 4.2 Hz, 1H), 7.32 (d, *J* = 3.6 Hz, 1H), 7.57 (d, *J* = 9.9 Hz, 2H), 7.77 (d, 1H), 7.96 (d, *J* = 2.1 Hz, 1H). EI-MS *m/z* 526 (M<sup>+</sup>) 292 (100%). HRMS (EI) *m/z* calcd for C<sub>26</sub>H<sub>23</sub>ClN<sub>2</sub>O<sub>6</sub>S (M<sup>+</sup>) 526.0965, found 526.0972.

**2-Chloro-5-{5-[3-(2-methoxy-ethyl)-2-(4-methoxy-phenylimino)-4-oxo-thiazolidin-5-ylidenemethyl]-furan-2-yl}-benzoic Acid (4e).** In the same manner as described in the preparation of **2**, **4e** was prepared from 2-chloro-5-{5-[3-(2-methoxy-ethyl)-2-(4-methoxy-phenylimino)-4-oxo-thiazolidin-5-ylidenemethyl]-furan-2-yl}-benzoic acid methyl ester (**4d**). Yield: 89.9%. HPLC: 97.53%, *t*<sub>R</sub> = 4.30 min, mp 202–205 °C. <sup>1</sup>H NMR (DMSO-*d*<sub>6</sub>): δ 3.29 (s, 3H), 3.67 (t, *J* = 11.4 Hz, 3H), 3.81 (s, 3H), 4.05 (t, 2H), 7.04 (s, 4H), 7.11 (d, *J* = 3.6 Hz, 1H), 7.30 (d, *J* = 3.6 Hz, 1H), 7.49 (d, *J* = 8.4 Hz, 1H), 7.56 (s, 1H), 7.63 (d, *J* = 2.4 Hz, 1H), 7.98 (d, *J* = 2.1 Hz, 1H). EI-MS *m/z* 512 (M<sup>+</sup>) 278 (100%). HRMS (EI) *m/z* calcd for C<sub>25</sub>H<sub>21</sub>ClN<sub>2</sub>O<sub>6</sub>S (M<sup>+</sup>) 512.0813, found 512.0809.

**5-{5-[2-(4-Bromo-phenylimino)-3-(2-methoxy-ethyl)-4-oxo-thiazolidin-5-ylidenemethyl]-furan-2-yl}-2-chloro-benzoic Acid Methyl Ester (4f).** In the same manner as described in the preparation of **4c**, **4f** was prepared from 2-(4-bromo-phenylimino)-3-(2-methoxy-ethyl)-thiazolidin-4-one (**16c**), 2-chloro-5-(5-formyl-furan-2-yl)-benzoic acid methyl ester (**19a**), and hexahydropyridine. Yield: 69.8%. HPLC: 100.00%, *t*<sub>R</sub> = 17.13 min, mp 151–153 °C. <sup>1</sup>H NMR (DMSO-*d*<sub>6</sub>): δ 3.29 (s, 3H), 3.68 (t, *J* = 11.1 Hz, 2H), 3.85 (s, 2H), 4.06 (t, 2H), 7.05 (s, 1H), 7.08 (s, 1H), 7.19 (d, *J* = 3.3 Hz, 1H), 7.38 (d, *J* = 3.6 Hz, 1H), 7.61–7.65 (m, 4H), 7.82 (d, *J* = 2.1 Hz, 1H), 8.04 (d, *J* = 2.7 Hz, 1H). EI-MS *m/z* 574 (M<sup>+</sup>) 292 (100%); HRMS (EI) *m/z* calcd for C<sub>25</sub>H<sub>20</sub>BrClN<sub>2</sub>O<sub>5</sub>S (M<sup>+</sup>) 573.9956, found 573.9965.

**5-{5-[2-(2-Bromo-phenylimino)-3-(2-methoxy-ethyl)-4-oxo-thiazolidin-5-ylidenemethyl]-furan-2-yl}-2-chloro-benzoic Acid Methyl Ester (4g).** In the same manner as described in the preparation of **4c**, **4g** was prepared from 2-(2-bromo-phenylimino)-3-(2-methoxy-ethyl)-thiazolidin-4-one (**16m**), 2-chloro-5-(5-formyl-furan-2-yl)-benzoic acid methyl ester (**19a**), and hexahydropyridine. Yield: 62.5%. HPLC: 96.12%, *t*<sub>R</sub> = 11.49 min, mp 145–146 °C. <sup>1</sup>H NMR (DMSO-*d*<sub>6</sub>): δ 3.30 (s, 3H), 3.78 (t, *J* = 11.1 Hz, 2H), 3.82 (s, 3H), 4.10 (t, *J* = 11.1 Hz, 2H), 7.18–7.23 (m, 3H), 7.37 (d, *J* = 9.6 Hz, 1H), 7.47 (m, 1H), 7.58 (d, 1H), 7.65 (s, 1H), 7.75–7.786 (m, 2H), 7.94 (d, *J* = 2.7 Hz, 1H). EI-MS *m/z* 574 (M<sup>+</sup>) 292 (100%); HRMS (EI) *m/z* calcd for C<sub>25</sub>H<sub>20</sub>BrClN<sub>2</sub>O<sub>5</sub>S (M<sup>+</sup>) 573.9939, found 573.9965.

**5-{5-[2-(3-Bromo-phenylimino)-3-(2-methoxy-ethyl)-4-oxo-thiazolidin-5-ylidenemethyl]-furan-2-yl}-2-chloro-benzoic Acid Methyl Ester (4h).** In the same manner as described in the preparation of **4c**, **4h** was prepared from 2-(3-bromo-phenylimino)-3-(2-methoxy-ethyl)-thiazolidin-4-one (**16n**), 2-chloro-5-(5-formyl-furan-2-yl)-benzoic acid methyl ester (**19a**), and hexahydropyridine. Yield: 65.0%. HPLC: 100.00%, *t*<sub>R</sub> = 16.39 min, mp 120–122 °C. <sup>1</sup>H NMR (DMSO-*d*<sub>6</sub>): δ 3.29 (s, 3H), 3.67 (t, *J* = 12.0 Hz, 2H), 3.82 (s, 3H), 4.06 (t, *J* = 11.4 Hz, 2H), 7.10 (d, *J* = 7.5 Hz, 1H), 7.18 (d, *J* = 3.9 Hz, 1H), 7.31–7.37 (m, 2H), 7.41–7.44 (m, 2H), 7.58–7.63 (m, 2H), 7.77 (dd, *J* = 2.1 Hz and *J* = 2.1 Hz, 1H), 8.01 (d, *J* = 2.1 Hz, 1H). EI-MS *m/z* 574 (M<sup>+</sup>) 292 (100%). HRMS (EI) *m/z* calcd for C<sub>25</sub>H<sub>20</sub>BrClN<sub>2</sub>O<sub>5</sub>S (M<sup>+</sup>) 573.9971, found 573.9965.

**2-Chloro-5-{5-[3-(2-methoxy-ethyl)-2-(naphthalen-1-ylimino)-4-oxo-thiazolidin-5-ylidenemethyl]-furan-2-yl}-benzoic Acid Methyl Ester (4i).** In the same manner as described in the preparation of **4c**, **4i** was prepared from 3-(2-methoxy-ethyl)-2-(naphthalen-1-ylimino)-thiazolidin-4-one (**16d**), 2-chloro-5-(5-formyl-furan-2-yl)-benzoic acid methyl ester (**19a**), and hexahydropyridine. Yield: 62.3%. HPLC: 100.00%, *t*<sub>R</sub> = 16.27 min, mp 126–128 °C. <sup>1</sup>H NMR (DMSO-*d*<sub>6</sub>): δ 3.36 (s, 3H), 3.73 (s, 2H), 3.80 (t, *J* = 11.1 Hz, 2H), 4.22 (t, 2H), 7.09 (d, *J* = 3.9 Hz, 1H), 7.19 (d, *J* = 6.9 Hz, 1H), 7.27 (d, *J* = 3.6 Hz, 1H), 7.50–7.59 (m, 5H), 7.65 (d, *J* = 2.1 Hz, 1H), 7.80–7.87 (m, 3H), 7.97 (t, *J* = 6.9 Hz, 2H). EI-MS *m/z* 546 (M<sup>+</sup>) 292 (100%). HRMS (EI) *m/z* calcd for C<sub>29</sub>H<sub>23</sub>ClN<sub>2</sub>O<sub>5</sub>S (M<sup>+</sup>) 546.1019, found 546.1016.

**2-Chloro-5-{5-[3-(2-methoxy-ethyl)-2-(naphthalen-1-ylimino)-4-oxo-thiazolidin-5-ylidenemethyl]-furan-2-yl}-benzoic Acid (4j).** In the same manner as described in the preparation of **2**, **4j** was prepared from 2-chloro-5-{5-[3-(2-methoxy-ethyl)-2-(naphthalen-1-ylimino)-4-oxo-thiazolidin-5-ylidenemethyl]-furan-2-yl}-benzoic acid methyl ester (**4i**). Yield: 90.1%. HPLC: 97.98%, *t*<sub>R</sub> = 7.41

min, mp 230–231 °C. <sup>1</sup>H NMR (DMSO-*d*<sub>6</sub>): δ 3.36 (s, 3H), 3.81 (t, *J* = 5.1 Hz, 2H), 4.24 (t, 2H), 7.10 (d, *J* = 3.6 Hz, 1H), 7.23 (d, 1H), 7.28 (d, *J* = 3.9 Hz, 1H), 7.47–7.61 (m, 6H), 7.80–7.88 (m, 2H), 7.98 (t, 2H). ESI-MS *m/z* 532 [M + H]<sup>+</sup>. HRMS (ESI) *m/z* calcd for C<sub>28</sub>H<sub>21</sub>ClN<sub>2</sub>O<sub>5</sub>Na [M + Na]<sup>+</sup> 555.0732, found 555.0757.

**2-Chloro-5-{5-[3-(2-methoxy-ethyl)-4-oxo-2-(4-trifluoromethyl-phenylimino)-thiazolidin-5-ylidenemethyl]-furan-2-yl}-benzoic Acid Methyl Ester (4k).** In the same manner as described in the preparation of **4c**, **4k** was prepared from 3-(2-methoxy-ethyl)-2-(4-trifluoromethyl-phenylimino)-thiazolidin-4-one (**16e**), 2-chloro-5-(5-formyl-furan-2-yl)-benzoic acid methyl ester (**19a**), and hexahydropyridine. Yield: 64.1%. HPLC: 98.08%, *t*<sub>R</sub> = 14.52 min, mp 155–157 °C. <sup>1</sup>H NMR (DMSO-*d*<sub>6</sub>): δ 3.30 (s, 3H), 3.69 (t, *J* = 11.4 Hz, 2H), 3.79 (s, 2H), 4.08 (t, *J* = 11.7 Hz, 2H), 7.18 (d, *J* = 3.6 Hz, 1H), 7.28 (d, *J* = 4.8 Hz, 2H), 7.35 (d, *J* = 2.4 Hz, 1H), 7.50 (d, 1H), 7.63 (s, 1H), 7.73 (dd, *J* = 1.8 Hz and *J* = 2.4 Hz, 1H), 7.82 (d, *J* = 8.7 Hz, 2H), 8.02 (d, *J* = 1.8 Hz, 1H). EI-MS *m/z* 564 (M<sup>+</sup>) 292 (100%). HRMS (EI) *m/z* calcd for C<sub>26</sub>H<sub>20</sub>ClF<sub>3</sub>N<sub>2</sub>O<sub>5</sub>S (M<sup>+</sup>) 564.0739, found 564.0734.

**2-Chloro-5-{5-[3-(2-methoxy-ethyl)-4-oxo-2-(2-trifluoromethyl-phenylimino)-thiazolidin-5-ylidenemethyl]-furan-2-yl}-benzoic Acid Methyl Ester (4l).** In the same manner as described in the preparation of **4c**, **4l** was prepared from 3-(2-methoxy-ethyl)-2-(2-trifluoromethyl-phenylimino)-thiazolidin-4-one (**16k**), 2-chloro-5-(5-formyl-furan-2-yl)-benzoic acid methyl ester (**19a**), and hexahydropyridine. Yield: 65.6%. HPLC: 98.23%, *t*<sub>R</sub> = 10.40 min, mp 141–143 °C. <sup>1</sup>H NMR (DMSO-*d*<sub>6</sub>): δ 3.27 (s, 3H), 3.70 (t, *J* = 11.1 Hz, 2H), 3.81 (s, 3H), 4.07 (t, *J* = 11.7 Hz, 2H), 7.19 (d, *J* = 3.6 Hz, 1H), 7.27 (d, 1H), 7.35 (d, *J* = 3.9 Hz, 1H), 7.45 (m, 1H), 7.58 (d, 1H), 7.66 (s, 1H), 7.72–7.82 (m, 3H), 7.93 (d, *J* = 1.8 Hz, 1H). EI-MS *m/z* 564 (M<sup>+</sup>) 292 (100%). HRMS (EI) *m/z* calcd for C<sub>26</sub>H<sub>20</sub>ClF<sub>3</sub>N<sub>2</sub>O<sub>5</sub>S (M<sup>+</sup>) 564.0737, found 564.0734.

**2-Chloro-5-{5-[3-(2-methoxy-ethyl)-4-oxo-2-(3-trifluoromethyl-phenylimino)-thiazolidin-5-ylidenemethyl]-furan-2-yl}-benzoic Acid Methyl Ester (4m).** In the same manner as described in the preparation of **4c**, **4m** was prepared from 3-(2-methoxy-ethyl)-2-(3-trifluoromethyl-phenylimino)-thiazolidin-4-one (**16l**), 2-chloro-5-(5-formyl-furan-2-yl)-benzoic acid methyl ester (**19a**), and hexahydropyridine. Yield: 60.3%. HPLC: 96.60%, *t*<sub>R</sub> = 13.76 min, mp 92–95 °C. <sup>1</sup>H NMR (DMSO-*d*<sub>6</sub>): δ 3.30 (s, 3H), 3.69 (t, *J* = 11.1 Hz, 2H), 3.78 (s, 3H), 4.07 (t, *J* = 11.1 Hz, 2H), 7.15 (d, *J* = 3.6 Hz, 1H), 7.32 (d, *J* = 3.6 Hz, 1H), 7.40–7.42 (m, 2H), 7.47–7.49 (m, 1H), 7.60–7.62 (m, 2H), 7.66–7.69 (m, 2H), 7.96 (d, *J* = 2.1 Hz, 1H). EI-MS *m/z* 564 (M<sup>+</sup>) 292 (100%). HRMS (EI) *m/z* calcd for C<sub>26</sub>H<sub>20</sub>ClF<sub>3</sub>N<sub>2</sub>O<sub>5</sub>S (M<sup>+</sup>) 564.0741, found 564.0734.

**2-Chloro-5-{5-[3-(2-methoxy-ethyl)-2-(2-methoxy-phenylimino)-4-oxo-thiazolidin-5-ylidenemethyl]-furan-2-yl}-benzoic Acid Methyl Ester (4n).** In the same manner as described in the preparation of **4c**, **4n** was prepared from 3-(2-methoxy-ethyl)-2-(2-methoxy-phenylimino)-thiazolidin-4-one (**16i**), 2-chloro-5-(5-formyl-furan-2-yl)-benzoic acid methyl ester (**19a**), and hexahydropyridine. Yield: 63.4%. HPLC: 97.24%, *t*<sub>R</sub> = 6.50 min, mp 150–152 °C. <sup>1</sup>H NMR (DMSO-*d*<sub>6</sub>): δ 3.29 (s, 3H), 3.71 (t, *J* = 11.4 Hz, 2H), 3.76 (s, 3H), 3.83 (s, 3H), 4.08 (t, *J* = 11.4 Hz, 2H), 6.97–7.00 (m, 2H), 7.11–7.14 (m, 2H), 7.25 (m, 1H), 7.33 (d, *J* = 3.6 Hz, 1H), 7.56–7.59 (m, 2H), 7.74 (m, 1H), 7.94 (d, *J* = 1.8 Hz, 1H). EI-MS *m/z* 526 (M<sup>+</sup>) 292 (100%). HRMS (EI) *m/z* calcd for C<sub>26</sub>H<sub>23</sub>ClN<sub>2</sub>O<sub>6</sub>S (M<sup>+</sup>) 526.0968, found 526.0965.

**2-Chloro-5-{5-[3-(2-methoxy-ethyl)-2-(3-methoxy-phenylimino)-4-oxo-thiazolidin-5-ylidenemethyl]-furan-2-yl}-benzoic Acid Methyl Ester (4o).** In the same manner as described in the preparation of **4c**, **4o** was prepared from 3-(2-methoxy-ethyl)-2-(3-methoxy-phenylimino)-thiazolidin-4-one (**16j**), 2-chloro-5-(5-formyl-furan-2-yl)-benzoic acid methyl ester (**19a**), and hexahydropyridine. Yield: 66.7%. HPLC: 97.50%, *t*<sub>R</sub> = 8.56 min, mp 131–132 °C. <sup>1</sup>H NMR (DMSO-*d*<sub>6</sub>): δ 3.29 (s, 3H), 3.68 (t, *J* = 11.4 Hz, 2H), 3.76 (s, 3H), 3.81 (s, 3H), 4.06 (t, *J* = 11.4 Hz, 2H), 6.64 (dt, *J* = 3.9 Hz and *J* = 1.2 Hz, 2H), 6.80–6.83 (m, 1H), 7.13 (d, *J* = 3.6 Hz, 1H), 7.33–7.38 (m, 2H), 7.57–7.58 (m, 2H), 7.77 (dd, *J* = 2.1 Hz and *J* = 2.1 Hz, 1H), 7.97 (d, *J* = 2.1 Hz, 1H). EI-MS *m/z* 526

(M<sup>+</sup>) 292 (100%). HRMS (EI) *m/z* calcd for C<sub>26</sub>H<sub>23</sub>ClN<sub>2</sub>O<sub>6</sub>S (M<sup>+</sup>) 526.0965, found 526.0958.

**2-Chloro-5-{5-[2-(4-fluoro-phenylimino)-3-(2-methoxy-ethyl)-4-oxo-thiazolidin-5-ylidenemethyl]-furan-2-yl}-benzoic Acid Methyl Ester (4p).** In the same manner as described in the preparation of **4c**, **4p** was prepared from 2-(4-fluoro-phenylimino)-3-(2-methoxy-ethyl)-thiazolidin-4-one (**16p**), 2-chloro-5-(5-formyl-furan-2-yl)-benzoic acid methyl ester (**19a**), and hexahydropyridine. Yield: 60.2%. HPLC: 96.94%, *t*<sub>R</sub> = 9.26 min, mp 119–120 °C. <sup>1</sup>H NMR (DMSO-*d*<sub>6</sub>): δ 3.29 (s, 3H), 3.68 (t, *J* = 10.8 Hz, 2H), 3.83 (s, 3H), 4.05 (t, 2H), 7.10–7.13 (m, 2H), 7.17 (dd, *J* = 1.2 Hz, *J* = 1.2 Hz, 1H), 7.25–7.29 (m, 2H), 7.36 (dd, *J* = 1.5 Hz, *J* = 1.5 Hz, 1H), 7.60–7.63 (m, 2H), 7.81 (d, 1H), 7.96 (d, *J* = 1.8 Hz, 1H). EI-MS *m/z* 514 (M<sup>+</sup>) 292 (100%). HRMS (EI) *m/z* calcd for C<sub>25</sub>H<sub>20</sub>ClF<sub>2</sub>N<sub>2</sub>O<sub>5</sub>S (M<sup>+</sup>) 514.0762, found 514.0765.

**2-Chloro-5-{5-[2-(3-fluoro-phenylimino)-3-(2-methoxy-ethyl)-4-oxo-thiazolidin-5-ylidenemethyl]-furan-2-yl}-benzoic Acid Methyl Ester (4q).** In the same manner as described in the preparation of **4c**, **4q** was prepared from 2-(3-fluoro-phenylimino)-3-(2-methoxy-ethyl)-thiazolidin-4-one (**16q**), 2-chloro-5-(5-formyl-furan-2-yl)-benzoic acid methyl ester (**19a**), and hexahydropyridine. Yield: 65.7%. HPLC: 95.15%, *t*<sub>R</sub> = 9.54 min, mp 126–128 °C. <sup>1</sup>H NMR (DMSO-*d*<sub>6</sub>): δ 3.29 (s, 3H), 3.68 (t, *J* = 11.7 Hz, 2H), 3.82 (s, 3H), 4.06 (t, *J* = 11.7 Hz, 2H), 6.92–6.96 (m, 2H), 7.05–7.12 (m, 1H), 7.18 (d, *J* = 3.9 Hz, 1H), 7.36 (d, *J* = 3.9 Hz, 1H), 7.50–7.53 (m, 1H), 7.59–7.63 (m, 2H), 7.81 (dd, *J* = 2.1 Hz and *J* = 2.1 Hz, 1H), 7.97 (d, *J* = 2.4 Hz, 1H). EI-MS *m/z* 514 (M<sup>+</sup>) 292 (100%). HRMS (EI) *m/z* calcd for C<sub>25</sub>H<sub>20</sub>ClF<sub>2</sub>N<sub>2</sub>O<sub>5</sub>S (M<sup>+</sup>) 514.0759, found 514.0765.

**2-Chloro-5-{5-[2-(2-fluoro-phenylimino)-3-(2-methoxy-ethyl)-4-oxo-thiazolidin-5-ylidenemethyl]-furan-2-yl}-benzoic Acid Methyl Ester (4r).** In the same manner as described in the preparation of **4c**, **4r** was prepared from 2-(2-fluoro-phenylimino)-3-(2-methoxy-ethyl)-thiazolidin-4-one (**16o**), 2-chloro-5-(5-formyl-furan-2-yl)-benzoic acid methyl ester (**19a**), and hexahydropyridine. Yield: 68.3%; mp 129–132 °C. <sup>1</sup>H NMR (DMSO-*d*<sub>6</sub>): δ 3.28 (s, 3H), 3.70 (t, *J* = 10.8 Hz, 2H), 3.82 (s, 3H), 4.09 (t, *J* = 11.1 Hz, 2H), 7.19 (d, *J* = 3.6 Hz, 2H), 7.26–7.37 (m, 4H), 7.60 (d, *J* = 8.1 Hz, 1H), 7.65 (s, 1H), 7.78 (dd, *J* = 2.1 Hz and *J* = 2.1 Hz, 1H), 7.96 (d, *J* = 2.1 Hz, 1H). EI-MS *m/z* 514 (M<sup>+</sup>) 292 (100%). HRMS (EI) *m/z* calcd for (M<sup>+</sup>) 514.0775, found 514.0765. Anal. (C<sub>25</sub>H<sub>20</sub>ClF<sub>2</sub>N<sub>2</sub>O<sub>5</sub>S) calcd, C 58.31, H 3.91, N 5.44; found C 58.15, H 3.83, N 5.28.

**2-Chloro-5-{5-[3-(3-dimethylamino-propyl)-4-oxo-2-phenylimino-thiazolidin-5-ylidenemethyl]-furan-2-yl}-benzoic Acid Methyl Ester (4s).** In the same manner as described in the preparation of **4c**, **4s** was prepared from 3-(3-dimethylamino-propyl)-2-phenylimino-thiazolidin-4-one (**16f**), 2-chloro-5-(5-formyl-furan-2-yl)-benzoic acid methyl ester (**19a**), and hexahydropyridine. Yield: 67.5%. HPLC: 96.26%, *t*<sub>R</sub> = 2.15 min, mp 134–136 °C. <sup>1</sup>H NMR (DMSO-*d*<sub>6</sub>): δ 1.83 (t, 2H), 2.13 (s, 6H), 2.29 (t, *J* = 6.3 Hz, 2H), 3.81 (s, 3H), 3.90 (t, *J* = 7.5 Hz, 2H), 7.06 (d, *J* = 7.2 Hz, 2H), 7.10 (d, *J* = 3.6 Hz, 1H), 7.24 (m, 1H), 7.31 (d, *J* = 3.6 Hz, 1H), 7.45 (m, 2H), 7.55 (t, 2H), 7.71 (d, *J* = 2.1 Hz, 2H), 7.93 (d, *J* = 2.4 Hz, 1H). EI-MS *m/z* 523 (M<sup>+</sup>) 84 (100%). HRMS (EI) *m/z* calcd for C<sub>27</sub>H<sub>26</sub>ClN<sub>3</sub>O<sub>4</sub>S (M<sup>+</sup>) 523.1337, found 523.1333.

**2-Chloro-5-{5-[3-(2-diethylamino-ethyl)-4-oxo-2-phenylimino-thiazolidin-5-ylidenemethyl]-furan-2-yl}-benzoic Acid Methyl Ester (4t).** In the same manner as described in the preparation of **4c**, **4t** was prepared from 3-(2-diethylamino-ethyl)-2-phenylimino-thiazolidin-4-one (**16g**), 2-chloro-5-(5-formyl-furan-2-yl)-benzoic acid methyl ester (**19a**), and hexahydropyridine. Yield: 64.9%. HPLC: 95.32%, *t*<sub>R</sub> = 2.06 min, mp 103–105 °C. <sup>1</sup>H NMR (DMSO-*d*<sub>6</sub>): δ 0.99 (t, *J* = 14.1 Hz, 6H), 2.59 (q, 4H), 2.87 (t, 2H), 3.82 (s, 3H), 3.99 (t, *J* = 12.6 Hz, 2H), 7.10 (d, *J* = 7.8 Hz, 3H), 7.14 (d, *J* = 3.9 Hz, 1H), 7.25 (t, 1H), 7.33 (d, *J* = 3.6 Hz, 2H), 7.46 (t, 2H), 7.56–7.59 (m, 2H), 7.76 (dd, *J* = 2.1 Hz and *J* = 2.1 Hz, 1H), 7.95 (d, *J* = 2.1 Hz, 1H). EI-MS *m/z* 537 (M<sup>+</sup>) 99 (100%). HRMS (EI) *m/z* calcd for C<sub>28</sub>H<sub>28</sub>ClN<sub>3</sub>O<sub>4</sub>S (M<sup>+</sup>) 537.1471, found 537.1489.

**2-Chloro-5-[5-[4-oxo-2-phenylimino-3-(2-pyrrolidin-1-yl-ethyl)-thiazolidin-5-ylidenemethyl]-furan-2-yl]-benzoic Acid Methyl Ester (4u).** In the same manner as described in the preparation of **4c**, **4u** was prepared from 2-phenylimino-3-(2-pyrrolidin-1-yl-ethyl)-thiazolidin-4-one (**16h**), 2-chloro-5-(5-formyl-furan-2-yl)-benzoic acid methyl ester (**19a**), and hexahydropyridine. Yield: 55.2%. HPLC: 95.98%,  $t_R = 2.07$  min, mp 110–112 °C.  $^1\text{H NMR}$  (DMSO- $d_6$ ):  $\delta$  1.90 (m, 4H), 2.90 (m, 4H), 3.11 (t, 2H), 3.87 (s, 3H), 4.10 (t,  $J = 6.9$  Hz, 2H), 6.92 (d,  $J = 3.6$  Hz, 1H), 7.05–7.11 (m, 2H), 7.25 (m, 1H), 7.40–7.44 (m, 4H), 7.47 (s, 1H), 7.62 (d,  $J = 2.4$  Hz, 1H), 7.97 (d,  $J = 2.1$  Hz, 1H). EI-MS  $m/z$  535 ( $M^+$ ) 97 (100%). HRMS (EI)  $m/z$  calcd for  $C_{28}H_{26}ClN_3O_4S$  ( $M^+$ ) 535.1314, found 535.1333.

**4-Chloro-3-[5-[3-(2-methoxy-ethyl)-4-oxo-2-phenylimino-thiazolidin-5-ylidenemethyl]-furan-2-yl]-benzoic Acid Methyl Ester (4a).** In the same manner as described in the preparation of **4c**, **4a** was prepared from 3-(2-methoxy-ethyl)-2-phenylimino-thiazolidin-4-one (**16a**), 4-chloro-3-(5-formyl-furan-2-yl)-benzoic acid methyl ester (**19b**), and hexahydropyridine. Yield: 66.3%. HPLC: 100.00%,  $t_R = 14.19$  min, mp 111–113 °C.  $^1\text{H NMR}$  (DMSO- $d_6$ ):  $\delta$  3.30 (s, 3H), 3.69 (t,  $J = 11.7$  Hz, 2H), 3.79 (s, 3H), 4.07 (t, 2H), 7.06 (d,  $J = 7.5$  Hz, 2H), 7.17–7.19 (m, 2H), 7.38–7.43 (m, 3H), 7.62 (s, 1H), 7.69–7.71 (d,  $J = 8.4$  Hz, 1H), 7.84–7.88 (m, 1H), 8.28 (d,  $J = 2.1$  Hz, 1H). EI-MS  $m/z$  496 ( $M^+$ ) 292 (100%). HRMS (EI)  $m/z$  calcd for  $C_{25}H_{21}ClN_2O_5S$  ( $M^+$ ) 496.0858, found 496.0860.

**5-[5-(4-Chloro-phenyl)-furan-2-ylmethylene]-3-(2-methoxy-ethyl)-2-phenylimino-thiazolidin-4-one (4b).** In the same manner as described in the preparation of **4c**, **4b** was prepared from 3-(2-methoxy-ethyl)-2-phenylimino-thiazolidin-4-one (**16a**), 5-(4-chlorophenyl)-furan-2-carbaldehyde (**19c**), and hexahydropyridine. Yield: 64.9%. HPLC: 96.29%,  $t_R = 13.03$  min, mp 176–178 °C.  $^1\text{H NMR}$  (DMSO- $d_6$ ):  $\delta$  3.30 (s, 3H), 3.70 (t,  $J = 5.7$  Hz, 2H), 4.07 (t,  $J = 6.3$  Hz, 2H), 7.08–7.14 (m, 3H), 7.26–7.28 (m, 2H), 7.43–7.51 (m, 4H), 7.59–7.64 (m, 3H). EI-MS  $m/z$  438 ( $M^+$ ) 234 (100%). HRMS (EI)  $m/z$  calcd for  $C_{23}H_{19}ClN_2O_3S$  ( $M^+$ ) 438.0811, found 438.0805.

**Bioassay. Enzymatic Inhibition Assay.** The enzymatic inhibition assay of *HpFabZ* was monitored by the spectrophotometric method as described previously.<sup>21,25</sup> In brief, the activity of *HpFabZ* was measured by detection of the decrease in absorbance at 260 nm for the conversion of crotonoyl-CoA to  $\beta$ -hydroxybutyryl-CoA. The compounds dissolved in 1% DMSO were incubated with the enzyme for 1 h before the assays were started. The 50% inhibitory concentration (IC<sub>50</sub>) of each inhibitor was estimated by fitting the inhibition data to a dose-dependent curve using a logistic derivative equation.<sup>41</sup>

**Anti-*H. pylori* Activity Assay.** The bacterial growth inhibition activity for the compounds was evaluated by using Paper Disc Method. Dimethyl sulfoxide and ampicillin paper were used as negative and positive control respectively. The minimum inhibitory concentrations (MIC) values were determined by the standard agar dilution method<sup>42</sup> using Columbia agar supplemented with 10% sheep blood containing 2-fold serial dilutions of agents. Bacterial suspension of *H. pylori* was made by swabbing and suspending the cells in sterile saline with a turbidity equivalent to a 2.0 McFarland standard. Compound-free Columbia agar media were used as controls. Inoculated plates were incubated at 37 °C under microaerobic conditions (85% N<sub>2</sub>, 10% CO<sub>2</sub> and 5% O<sub>2</sub>) and examined after 3 days. The MIC was generally defined as the lowest concentration of antimicrobial agent that completely inhibits visible bacterial growth.

**Crystallization and Data Collection.** The crystals of *HpFabZ* were obtained as described previously,<sup>24</sup> and then soaked by adding a final concentration of ~20 mM inhibitors for 24 h. Diffraction data was collected at 100K using Cu K $\alpha$  X-ray with a Rigaku R-Axis IV++ image plate. Before crystals were flash-frozen in liquid nitrogen, the drop was dehydrated against 500  $\mu\text{L}$  reservoir solution containing 4.0 M sodium formate for 24 h. The data was processed using mosfilm program package.<sup>48</sup> Analysis of the diffraction data indicated that the crystals belong to space group  $P2_12_1$ . The crystallographic statistics are summarized in Tables

S4 and S5 in Supporting Information). The structures were solved by molecular replacement method with the crystal structure of *HpFabZ* as the search model (PDB code 2GLL) and refined by using the program CNS.<sup>49</sup> Electron density interpretation and model building were performed using the computer graphics program “coot”.<sup>50</sup>

**Acknowledgment.** We thank the Shanghai Supercomputing Center and Computer Network Information Center of Chinese Academy of Sciences for allocation of computing time. This work was supported by the National Natural Science Foundation of China (grants 20721003 and 20872153), International Collaboration Projects (grants 2007DFB30370 and 20720102040) and the 863 Hi-Tech Program of China (grants 2006AA020602).

**Supporting Information Available:** Figure S1 and Table S1 showing the binding energies (in kcal/mol) and actual ranks of the 280 compounds in focused combinatorial library; Figure S2 showing the stereo view of the omit electron density map contoured at 1.0  $\sigma$  around the inhibitors; Tables S2 and S3 listing the element analysis and the HPLC reports for the purity check of the active compounds 1–5, as measured in two different mobile phases; Tables S4 and S5 listing the summary of diffraction data and structure refinement statistics. This material is available free of charge via the Internet at <http://pubs.acs.org>.

## References

- Warren, J. R.; Marshall, B. J. Unidentified curved bacilli on gastric epithelium in active chronic gastritis. *Lancet* **1983**, *1*, 1273–1275.
- Marshall, B. J.; Warren, J. R. Unidentified curved bacilli in the stomach of patients with gastritis and peptic ulceration. *Lancet* **1984**, *1*, 1311–1315.
- Sander, J. O.; Philip, M. S. *Helicobacter pylori* infection as a cause of gastritis, duodenal ulcer, gastric cancer and nonulcer dyspepsia: a systematic overview. *Can. Med. Assoc. J.* **1994**, *150*, 177–185.
- Zhang, C.; Yamada, N.; Wu, Y. L.; Wen, M.; Matsuhisa, T.; Matsukura, N. *Helicobacter pylori* infection, glandular atrophy and intestinal metaplasia in superficial gastritis, gastric erosion, erosive gastritis, gastric ulcer and early gastric cancer. *World J. Gastroenterol.* **2005**, *11*, 791–796.
- Pakodi, F.; Abdel-Salam, O. M. E.; Debrenceni, A.; Mózsik, G. *Helicobacter pylori*. One bacterium and a broad spectrum of human disease! An overview. *J. Physiol. (Paris)* **2000**, *94*, 139–152.
- Konturek, J. W. Discovery by Jaworski of *Helicobacter pylori* and its pathogenetic role in peptic ulcer, gastritis and gastric cancer. *J. Physiol. Pharmacol.* **2003**, *54*, 23–41.
- Zhang, C.; Yamada, N.; Wu, Y. L.; Wen, M.; Matsuhisa, T.; Matsukura, N. *Helicobacter pylori* infection, glandular atrophy and intestinal metaplasia in superficial gastritis, gastric erosion, erosive gastritis, gastric ulcer and early gastric cancer. *World J. Gastroenterol.* **2005**, *11*, 791–796.
- Sander, J. O.; Philip, M. S. Indications for treatment of *Helicobacter pylori* infection: a systematic overview. *Can. Med. Assoc. J.* **1994**, *150*, 189–198.
- Dziewiszewski, J.; Jarosz, M. Guidelines in the medical treatment of *Helicobacter pylori* infection. *J. Physiol. Pharmacol.* **2006**, *57*, 143–154.
- Mirbagheri, S. A.; Hasibi, M.; Abouzari, M.; Rashidi, A. Triple, standard quadruple and ampicillin-sulbactam-based quadruple therapies for *H. pylori* eradication: a comparative three-armed randomized clinical trial. *World J. Gastroenterol.* **2006**, *14*, 4888–4891.
- Gerrits, M. M.; van Vliet, A. H.; Kuipers, E. J.; Kusters, J. G. *Helicobacter pylori* and antimicrobial resistance: molecular mechanisms and clinical implications. *Lancet Infect. Dis.* **2006**, *6*, 699–709.
- Wolle, K.; Malferteiner, P. Treatment of *Helicobacter pylori*. *Best Pract. Res., Clin. Gastroenterol.* **2007**, *21*, 315–324.
- Mégraud, F. Basis for the management of drug-resistant *Helicobacter pylori* infection. *Drugs* **2004**, *64*, 1893–1904.
- Graham, D. Y.; Shiotani, A. New concepts of resistance in the treatment of *Helicobacter pylori* infections. *Nat. Clin. Pract. Gastroenterol. Hepatol.* **2008**, *5*, 321–331.
- Leong, R. W.; Chan, F. K. Drug-induced side effects affecting the gastrointestinal tract. *Expert. Opin. Drug. Saf.* **2006**, *5*, 585–592.
- Imase, K.; Takahashi, M.; Tanaka, A.; Tokunaga, K.; Sugano, H.; Tanaka, M.; Ishida, H.; Kamiya, S.; Takahashi, S. Efficacy of *Clostridium butyricum* preparation concomitantly with *Helicobacter pylori* eradication therapy in relation to changes in the intestinal microbiota. *Microbiol. Immunol.* **2008**, *52*, 56–61.



- (17) Rock, C. O.; Cronan, J. E. *Escherichia coli* as a model for the regulation of dissociable (type II) fatty acid biosynthesis. *Biochim. Biophys. Acta.* **1996**, *1302*, 1–16.
- (18) Kostrewa, D.; Winkler, F. K.; Folkers, G.; Scapozza, L.; Perozzo, R. The crystal structure of PfFabZ, the unique beta-hydroxyacyl-ACP dehydratase involved in fatty acid biosynthesis of *Plasmodium falciparum*. *Protein Sci.* **2005**, *14*, 1570–1580.
- (19) White, S. W.; Zheng, J.; Zhang, Y. M. Rock. The structural biology of type II fatty acid biosynthesis. *Annu. Rev. Biochem.* **2005**, *74*, 791–831.
- (20) Nie, Z.; Perretta, C.; Lu, J.; Su, Y.; Margosiak, S.; Gajiwala, K. S.; Cortez, J.; Nikulin, V.; Yager, K. M.; Appelt, K.; Chu, S. Structure-based design, synthesis, and study of potent inhibitors of beta-ketoacyl-acyl carrier protein synthase III as potential antimicrobial agents. *J. Med. Chem.* **2005**, *48*, 1596–1609.
- (21) Liu, W.; Luo, C.; Han, C.; Peng, S.; Yang, Y.; Yue, J.; Shen, X.; Jiang, H. A new beta-hydroxyacyl-acyl carrier protein dehydratase (FabZ) from *Helicobacter pylori*: Molecular cloning, enzymatic characterization, and structural modeling. *Biochem. Biophys. Res. Commun.* **2005**, *333*, 1078–1086.
- (22) Sharma, S. K.; Kapoor, M.; Ramya, T. N.; Kumar, S.; Kumar, G.; Modak, R.; Sharma, S.; Surolia, N.; Surolia, A. Identification, characterization, and inhibition of *Plasmodium falciparum* beta-hydroxyacyl-acyl carrier protein dehydratase (FabZ). *J. Biol. Chem.* **2003**, *278*, 45661–45671.
- (23) Garwin, J. L.; Klages, A. L.; Cronan, J. E. Structural, enzymatic, and genetic studies of beta-ketoacyl-acyl carrier protein synthases I and II of *Escherichia coli*. *J. Biol. Chem.* **1980**, *255*, 11949–11956.
- (24) Tasdemir, D.; Lack, G.; Brun, R.; Rüedi, P.; Scapozza, L.; Perozzo, R. Inhibition of *Plasmodium falciparum* fatty acid biosynthesis: evaluation of FabG, FabZ, and FabI as drug targets for flavonoids. *J. Med. Chem.* **2006**, *49*, 3345–3353.
- (25) Zhang, L.; Liu, W.; Hu, T.; Du, L.; Luo, C.; Chen, K.; Shen, X.; Jiang, H. Structural basis for catalytic and inhibitory mechanisms of beta-hydroxyacyl-acyl carrier protein dehydratase (FabZ). *J. Biol. Chem.* **2008**, *283*, 5370–5379.
- (26) Chen, G.; Zheng, S.; Luo, X.; Shen, J.; Zhu, W.; Liu, H.; Gui, C.; Zhang, J.; Zheng, M.; Puah, C. M.; Chen, K.; Jiang, H. Focused combinatorial library design based on structural diversity, druglikeness and binding affinity score. *J. Comb. Chem.* **2005**, *7*, 398–406.
- (27) Zheng, S.; Luo, X.; Chen, G.; Zhu, W.; Shen, J.; Chen, K.; Jiang, H. A new rapid and effective chemistry space filter in recognizing a druglike database. *J. Chem. Inf. Model.* **2005**, *45*, 856–862.
- (28) Zhang, L.; Liu, W.; Xiao, J.; Hu, T.; Chen, J.; Chen, K.; Jiang, H.; Shen, X. Malonyl-CoA: acyl carrier protein transacylase from *Helicobacter pylori*: crystal structure and its interaction with acyl carrier protein. *Protein Sci.* **2007**, *16*, 1184–1192.
- (29) Hammam, A. E. G.; Abd El-Salam, O. I.; Mohamed, A. M.; Hafez, N. A. Novel fluoro substituted benzo[b]pyran with anti-lung cancer activity. *Indian. J. Chem., Sect. B: Org. Chem. Incl. Med. Chem.* **2005**, *35*, 1085–1087.
- (30) Keledjian, J.; Duffield, P. H.; Jamieson, D. D.; Lidgard, R. O.; Duffield, A. M. Uptake into mouse brain of four compounds present in the psychoactive beverage kava. *J. Pharm. Sci.* **1988**, *77*, 1003–1006.
- (31) Afarinkia, K.; Rees, C. W.; Cadogan, J. I. G. Synthesis of organophosphorus compounds via silyl esters of phosphorous acids. *Tetrahedron.* **1990**, *46*, 7175–7196.
- (32) Cho, J. K.; White, P. D.; Klute, W.; Dean, T. W.; Bradley, M. Self-indicating resins: sensor beads and in situ reaction monitoring. *J. Comb. Chem.* **2003**, *5*, 632–636.
- (33) Holla, B. S.; Malini, K. V.; Sarojini, B. K.; Poojary, B. A novel three-component synthesis of triazinothiazolones. *Synth. Commun.* **2005**, *35*, 333–340.
- (34) Ewing, T. J. A.; Kuntz, I. D. Critical evaluation of search algorithms for automated molecular docking and database screening. *J. Comput. Chem.* **1997**, *18*, 1175–1189.
- (35) Kuntz, I. D. Structure-based strategies for drug design and discovery. *Science* **1992**, *257*, 1078–1082.
- (36) Morris, G. M.; Goodsell, D. S.; Halliday, R. S.; Huey, R.; Hart, W. E.; Belew, R. K.; Olson, A. J. Automated docking using a Lamarckian genetic algorithm and an empirical binding free energy function. *J. Comput. Chem.* **1998**, *19*, 1639–1662.
- (37) Weiner, S. J.; Kollman, P. A.; Nguyen, D. T.; Case, D. A. An all atom force field for simulations of proteins and nucleic acids. *J. Comput. Chem.* **1986**, *7*, 230–252.
- (38) Gasteiger, J.; Marsili, M. Iterative partial equalization of orbital electronegativity—a rapid access to atomic charges. *Tetrahedron.* **1980**, *36*, 3219–3228.
- (39) Lipinski, C. A.; Lombardo, F.; Dominy, B. W.; Feeney, P. J. Experimental and computational approaches to estimate solubility and permeability in drug discovery and development settings. *Adv. Drug Delivery Rev.* **1997**, *23*, 3–25.
- (40) Zheng, S.; Luo, X.; Chen, G.; Zhu, W.; Shen, J.; Chen, K.; Jiang, H. A New Rapid and Effective Chemistry Space Filter in Recognizing a Druglike Database. *J. Chem. Inf. Model.* **2005**, *45*, 856–862.
- (41) Chen, L.; Gui, C.; Luo, X.; Yang, Q.; Gunther, S.; Scandella, E.; Drost, C.; Bai, D.; He, X.; Ludewig, B.; Chen, J.; Luo, H.; Yang, Y.; Yang, Y.; Zou, J.; Thiel, V.; Chen, K.; Shen, J.; Shen, X.; Jiang, H. Cinanserin is an inhibitor of the 3C-like proteinase of severe acute respiratory syndrome coronavirus and strongly reduces virus replication in vitro. *J. Virol.* **2005**, *79*, 7095–7103.
- (42) Osato, M. S. Antimicrobial susceptibility testing for *Helicobacter pylori*: sensitivity test results and their clinical relevance. *Curr. Pharm. Des.* **2000**, *6*, 1545–1555.
- (43) Schneider, G.; Böhm, H. J. Virtual screening and fast automated docking methods. *Drug Discovery Today* **2002**, *7*, 64–70.
- (44) Wang, R.; Lu, Y.; Wang, S. Comparative evaluation of 11 scoring functions for molecular docking. *J. Med. Chem.* **2003**, *46*, 2287–2303.
- (45) Nordfelth, R.; Kauppi, A. M.; Norberg, H. A.; Wolf-Watz, H.; Elofsson, M. Small-molecule inhibitors specifically targeting type III secretion. *Infect. Immun.* **2005**, *5*, 3104–3114.
- (46) Kirchhausen, T.; Macia, E.; Pelish, H. E. Use of dynasore, the small molecule inhibitor of dynamin, in the regulation of endocytosis. *Methods Enzymol.* **2008**, *438*, 77–93.
- (47) Zhang, J.; Pettersson, H. I.; Huitema, C.; Niu, C.; Yin, J.; James, M. N.; Eltis, L. D.; Vederas, J. C. Design, synthesis, and evaluation of inhibitors for severe acute respiratory syndrome 3C-like protease based on phthalhydrazide ketones or heteroaromatic esters. *J. Med. Chem.* **2007**, *50*, 1850–1864.
- (48) Lesslie, A. G. *Moslm User Guide: Moslm Version 5.2*; MRC Laboratory of Molecular Biology: Cambridge, UK, 1994.
- (49) Brünger, A. T.; Adams, P. D.; Clore, G. M.; DeLano, W. L.; Gros, P.; Grosse-Kunstleve, R. W.; Jiang, J. S.; Kuszewski, J.; Nilges, M.; Pannu, N. S.; Read, R. J.; Rice, L. M.; Simonson, T.; Warren, G. L. Crystallography and NMR system: a new software suite for macromolecular structure determination. *Acta Crystallogr., Sect. D: Biol. Crystallogr.* **1998**, *54*, 905–921.
- (50) Emsley, P.; Cowtan, K. Coot: model-building tools for molecular graphics. *Acta Crystallogr., Sect. D: Biol. Crystallogr.* **2004**, *60*, 2126–2132.
- (51) DeLano, W. L. The PyMOL Molecular Graphics System (2002) DeLano Scientific, Palo Alto, CA, USA. <http://www.pymol.org>.
- (52) Petrek, M.; Kosinova, P.; Koca, J.; Otyepka, M. MOLE: A Voronoi Diagram-Based Explorer of Molecular Channels, Pores, and Tunnels. *Structure.* **2007**, *15*, 1357–1363.

JM8015602